Journal of Vertebrate Paleontology e2616325 (19 pages)
Published with license by the Society of Vertebrate Paleontology
DOI: 10.1080/02724634.2026.2616325

ARTICLE

THE ONTOGENETICALLY YOUNGEST KNOWN PACHYCEPHALOSAUR (DINOSAURIA: ORNITHISCHIA) POSTCRANIUM

BRYAN R. S. MOORE,[1]* DAVID C. EVANS,[2,3] MICHAEL J. RYAN,[1,4] R. TIMOTHY PATTERSON,[1] and JORDAN C. MALLON[1,4]
[1]Ottawa Carleton Geoscience Center and Department of Earth Sciences, Carleton University, Ottawa, Ontario K1S 5B6, Canada, bryan.moore@ucalgary.ca, michaelj.ryan@carleton.ca, tim.patterson@carleton.ca;
[2]Department of Natural History, Royal Ontario Museum, Toronto, Ontario M5S 2C6, Canada, d.evans@utoronto.ca;
[3]Department of Ecology and Evolutionary Biology, University of Toronto, Toronto, Ontario M5S 3B2, Canada;
[4]Beaty Centre for Species Discovery and Paleobiology section, Canadian Museum of Nature, Ottawa, Ontario K1P 6P4, Canada, jmallon@nature.ca

ABSTRACT—Pachycephalosaurian dinosaurs are represented in the fossil record primarily by their taphonomically resistant frontoparietal domes that developed fully only at maturity. Consequently, the postcranial record of Pachycephalosauria is poor, particularly for immature forms. Here, we describe the ontogenetically youngest known, and Canada's second-most complete, pachycephalosaur postcranium, collected from the uppermost Maastrichtian Frenchman Formation, Saskatchewan. Despite its small size (estimated total length ~90 cm), the skeleton shows several characters diagnostic of Pachycephalosauria, including a double ridge-and-groove articulation on the pre- and postzygapophyses of the dorsal neural arches, a medial flange on the postacetabular process of the ilium, and a highly reduced pubis that contributes only minimally to the acetabular margin. Histological sectioning of the crural bones shows an immature woven bone texture. The absence of cyclical or annual growth indicators suggests that this specimen was less than a year old at the time of death. Phylogenetic analysis recovers the specimen as a member of Pachycephalosaurinae, perhaps related to *Prenocephale*, but the lack of cranial data for our specimen and the complementary lack of postcranial data for other pachycephalosaurs make this determination tenuous. Spatiotemporal considerations suggest a possible but currently untestable affiliation with *Sphaerotholus buchholtzae*. The relatively long hindlimbs of the juvenile compared with those of adult pachycephalosaurs indicate probable negative ontogenetic allometry in the hindlimbs.

SUPPLEMENTARY FILE(S)—Supplementary files are available for this article for free at www.tandfonline.com/UJVP.

Citation for this article: Moore, B. R. S., Evans, D. C., Ryan, M. J., Patterson, R. T., & Mallon, J. C. (2026) The ontogenetically youngest known pachycephalosaur (Dinosauria: Ornithischia) postcranium. *Journal of Vertebrate Paleontology*. 10.1080/02724634.2026.2616325

Submitted: February 3, 2025
Revisions received: December 12, 2025
Accepted: December 16, 2025

INTRODUCTION

Pachycephalosauria comprises mostly small (~2–6 m long), bipedal dinosaurs from the Santonian to Maastrichtian (85 to 66 Ma) of Asia and North America (Butler & Sullivan, 2009; Maryańska et al., 2004; Sereno, 1997). The clade is best known for the fusion of its frontal and parietal bones into an inflated dome. The surrounding cranial elements are sometimes incorporated into this structure and are often adorned with nodes, spikes, and other ornaments. Because the frontoparietal domes are the most taphonomically resistant parts of pachycephalosaur skeletons (except for teeth), the pachycephalosaurian fossil record is dominated by these partial cranial remains (Evans et al., 2013b; Mallon & Evans, 2014). As a result, much of what is known about pachycephalosaur ontogeny and phylogeny is based largely on skull morphology (Evans et al., 2013b).

Here, we describe a small partial skeleton representing the ontogenetically youngest known pachycephalosaur postcranium. The specimen (CMNFV 22039), consisting of several axial elements, the pelvis, and hindlimb material, was collected from the upper Maastrichtian Frenchman Formation of southern Saskatchewan in 1973. It was never described or illustrated but was originally assigned to *Thescelosaurus* sp. by Russell and Manabe (2002). Our taxonomic reinterpretation of CMNFV 22039 establishes it as Canada's second-most complete pachycephalosaur postcranium known to date (after UALVP 2, a largely complete skeleton of *Stegoceras validum* Lambe, 1902). In this study, we provide a comprehensive description of CMNFV 22039 and perform an osteohistological analysis to estimate the age-at-death of the specimen. Furthermore, we add CMNFV 22039,

*Corresponding author.

Color versions of one or more of the figures in the article can be found online at www.tandfonline.com/ujvp.

Published online 26 Feb 2026

along with new postcranial characters for other pachycephalosaurs, to the phylogenetic analysis of Chinzorig et al. (2025) to constrain the taxonomic identity of the specimen. We show that juvenile pachycephalosaurs likely exhibited compensatory locomotor performance compensation due to their relatively long distal hindlimbs compared with adults. CMNFV 22039 demonstrates that diagnostic features of the pachycephalosaur postcranium are largely conserved early in ontogeny, making it possible to identify their remains from isolated elements.

Regional Geology

CMNFV 22039 was found within the upper Maastrichtian (Upper Cretaceous) Frenchman Formation, the youngest of five Maastrichtian formations in southern Saskatchewan (Bamforth et al., 2014). The other four (from oldest to youngest: the marine Bearpaw Formation, the transitional Eastend Formation, and the terrestrial Whitemud and Battle formations) show evidence of regression of the Western Interior Sea throughout the Maastrichtian (Bamforth et al., 2014; Fraser et al., 1935; Furnival, 1946; Mossop & Shetsen, 1994). The Frenchman Formation disconformably overlies the Battle Formation in most exposures. It consists primarily of interbedded sandstones and claystones with occasional paleosols. Subsidence associated with orogenic activity in the Cordillera is thought to be responsible for the deposition of the Frenchman Formation (Catuneanu & Sweet, 1999; McIver, 2002), which was deposited in a low-lying system of meandering rivers and overbank settings (Bamforth et al., 2014; McIver, 2002). The top of the Frenchman Formation is marked by the Ferris coal seam, the lowest of several coals in the overlying Ravenscrag Formation (Bamforth et al., 2014; Fraser et al., 1935; Furnival, 1946; Kupsch, 1957; McIver, 2002). The K–Pg boundary typically occurs near the base of that coal. The Frenchman Formation has been dated to approximately 66.88–66.043 Ma, based on recent comparisons with the correlative lower Scollard Formation in Alberta (Eberth & Kamo, 2019).

An assortment of vertebrate macrofossils, microfossils, and invertebrate traces is preserved throughout the Frenchman Formation. Non-dinosaurian vertebrate fossils are represented by several species of fish, amphibians, freshwater turtles, squamates, choristoderes, crocodilians, and mammals (Bamforth *et al*., 2014; Brown *et al*., 2011; Storer, 1989; Tokaryk, 1997, 2009; Tokaryk & Brinkman, 2009; Tokaryk & Bryant, 2004; Tokaryk & James, 1989). Of the dinosaurs, *Triceratops prorsus* Marsh, 1890 is most common (Mallon et al., 2025; Tokaryk, 2009). Other dinosaur clades include thescelosaurids, hadrosaurids, ankylosaurids, tyrannosaurids, ornithomimids, caenagnathids, dromaeosaurids, troodontids, and birds (Brown et al., 2015; Tokaryk & Bryant, 2004). The pachycephalosaurid cf. *Sphaerotholus buchholtzae* Williamson & Carr, 2003 is represented in the Frenchman Formation by a single left postorbital (Mallon et al., 2015).

CMNFV 22039 Locality

CMNFV 22039 was discovered by Dale Russell in 1973 immediately outside what is now the East Block of Grasslands National Park (NW ¼ of the SE ¼, section 35, range 5, township 1, west of the 3rd meridian) (Fig. 1A). Russell's field notes (available in the CMNFV archives) report that the specimen was preserved at the base of a 7.0 m thick gray claystone unit of the Frenchman Formation, 17.8 m below the Ferris coal seam (Fig. 1B). The claystone unit is directly overlain by 4.5 m of sandy siltstone, followed by another 6.3 m of gray claystone, which is topped by the Ferris coal seam. A letter in the museum archives from Russell to Frank Simpson of the Subsurface Geological Laboratory in Regina, Saskatchewan (dated May 13, 1977) further states that the fossil was collected near the base of the local exposures. A team from the Canadian Museum of Nature, with help from local farmer Miles Anderson and Russell's original field assistant Gilles Danis (both of whom were present during the original collection of CMNFV 22039), attempted to relocate the original quarry in August 2021 and June 2025. Unfortunately, the team was unable to confidently relocate the quarry. However, examination of the surrounding geology showed localized, step-like slumping, resulting in the Ferris coal seam appearing approximately 18 m below its actual position. The coal seam is not exposed elsewhere in the area. As far as we can determine, Russell did not initially account for this slumping in his original geological column. Therefore, we estimate that the quarry was near the base of the Frenchman Formation (Fig. 1C, D), which is approximately 35 m thick in the East Block of Grasslands National Park (Bamforth, 2013).

Institutional Abbreviations—**CMNFV**, Canadian Museum of Nature (Fossil Vertebrates), Ottawa, Ontario, Canada; **MPC**, Palaeontological Center, Mongolian Academy of Sciences, Ulaanbaatar, Mongolia; **NSM PV**, National Science Museum, Tokyo, Japan; **ROM**, Royal Ontario Museum, Toronto, Ontario, Canada; **UALVP**, University of Alberta Laboratory for Vertebrate Paleontology, Edmonton, Alberta, Canada.

MATERIALS AND METHODS

Three-dimensional Modeling

We 3D-scanned the larger bones of CMNFV 22039 (including the crus, prior to histological thin-sectioning) using a Go!SCAN 20 portable scanner (Creaform, Lévis, Québec, Canada) at the Canadian Museum of Nature. Initial scan resolution was 0.3 mm. The resulting scan files were then imported into the associated VXelements v. 7.0.2 software for post-processing.

Elements that were too small for the portable scanner to detect (pubis, distal crural elements) were 3D-modeled using photogrammetry. Each element was photographed circumferentially, and each image series was then imported into Abound v. 3.0.1 (Abound Labs Inc., New York, NY, USA) to produce a photogrammetric model. The 3D models are available at: https://www.morphosource.org/projects/000731298.

Osteohistological Analysis

To determine the ontogenetic age of CMNFV 22039, we performed an osteohistological analysis of the left tibia and left fibula. Thin sections were made by first drawing a line at the approximate minimum circumference of the diaphyses to indicate the line of cut. Technovit 5071 was then applied around the line in a 2:1 powder-water ratio to stabilize the element for cutting. After the Technovit had cured, a transverse cut was made using a Buehler Isomet 1000 precision saw. After premount grinding, the surface to be joined to the slide was adhered to the frosted acrylic microscope slide using a cyanoacrylate adhesive. Once cured, the excess sample material was cut away from the slide using the same precision saw. Using a Hillquist thin section machine, the thin section was then ground down until light was visibly able to pass through it. The thin section was polished by hand using 600- and then 1000-grit silicon carbide mixtures. Finally, the completed thin sections were viewed and photomicrographed under a Nikon AZ100 microscope under both normal and cross-polarized light. Original high-resolution histological imagery is available in Supplementary File 1.

Phylogenetic Analysis

We conducted a parsimony-based cladistic analysis to aid in the taxonomic identification of CMNFV 22039, based on the

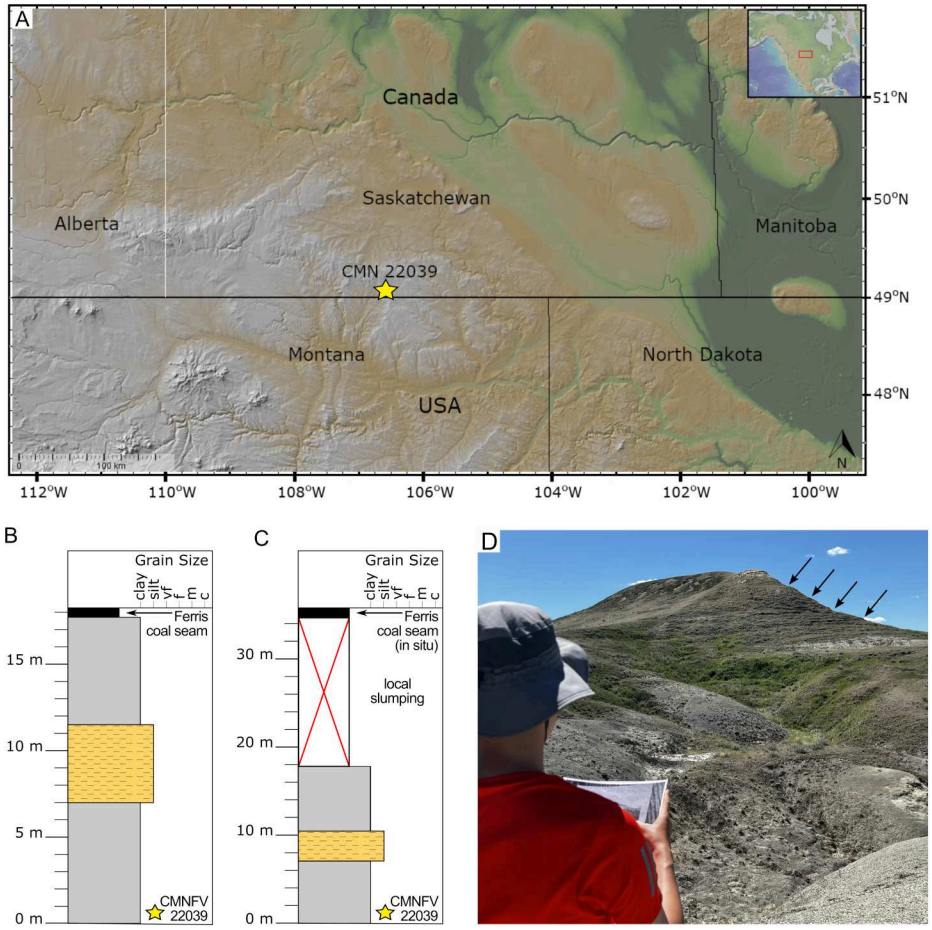

FIGURE 1. Geographic and stratigraphic context of juvenile Pachycephalosauria indet. (CMNFV 22039). **A**, map of southern Saskatchewan showing locality of specimen (star), created using GeoMapApp (www.geomapapp.org) (Ryan et al., 2009); **B**, local stratigraphic section showing the location of the specimen (star) based on D. Russell's 1973 field notes (Canadian Museum of Nature archives); **C**, revised local stratigraphic section showing the location of the specimen (star). The Ferris coal seam marks the base of the Ravenscrag Formation. **D**, photo showing stepped slumping (indicated by arrows) on hillside near quarry locality. The in situ Ferris coal seam occurs near the top of the hillside.

pachycephalosaurian character matrix of Chinzorig et al. (2025). We added two new postcranial characters of potential phylogenetic significance (Chs. 83 and 84). Character 83 concerns the projection angle of the medial flange of the ilium. In most pachycephalosaur ilia, the medial flange projects horizontally from the dorsal margin of the ilium (state 0). In *Steg. validum* (UALVP 2) and CMNFV 22039, however, the medial flange projects dorsomedially (state 1) (see 'Description of CMNFV 22039' below).

Character 84 concerns the shape of the femoral fourth trochanter. Among pachycephalosaurs, CMNFV 22039 and *Pr. prenes* exhibit a weakly pendant trochanter morphology (state 1), while others exhibit a non-pendant morphology (state 2) (see 'Description of CMNFV 22039' below). In marginocephalians, the ancestral condition is a strongly pendant fourth trochanter (state 0). Although the apex of the fourth trochanter of CMNFV 22039 is broken, it still clearly exhibits a pendant morphology compared with the non-pendant fourth trochanter of other pachycephalosaurs (e.g., *Steg. validum*, *Z. rinpoche*). It is possible that the fourth trochanter of CMNFV 22039 displayed the strongly pendant ancestral morphology; however, without the preserved apex, this is impossible to determine with certainty. This morphology does not appear to vary through ontogeny in at least some basally-branching marginocephalians, as the condition does not change in neonatal to adult specimens of *Protoceratops* (Fastovsky et al., 2011; Persons & Currie, 2020; Slowiak et al., 2019).

The final character matrix (Supplementary File 2) contained 23 operational taxonomic units and 85 characters and was 43.9% complete overall. Specimen CMNFV 22039 was scored for 12 characters (14.1% of the total). We analyzed the dataset in TNT v. 1.6 (Goloboff & Morales, 2023). Following Chinzorig et al. (2025), characters 1, 2, 8, 12, 26, 33, 34, 37, 48, 66, and 73 were treated as ordered, and *Psittacosaurus mongoliensis* was designated as the outgroup. The number of trees held in memory set to 500,000 using the "hold" command. We ran an implicit enumeration search using both equal character weighting and implied weighting (Goloboff et al., 2008) with a weighting function (k) of 12 (Goloboff et al., 2018). All other settings not mentioned here were left to their default values. Node support was estimated for the strict consensus trees using a standard bootstrap procedure, specifying 1000 replicates and a traditional search algorithm.

Analysis of Hindlimb Proportions

To understand how the hindlimb proportions of CMNFV 22039 compare to those of other pachycephalosaurs and bipedal ornithischians more broadly, we compiled a dataset of femur, tibia, and metatarsal III lengths for 45 taxa. Measurements were taken by us, by our colleagues, and from the literature. We sampled widely across Ornithischia, although we

focused primarily on small and mid-sized bipedal forms, including some large and/or facultative bipeds for comparison (raw measurements available in Supplementary File 3). We also included the quadrupedal thyreophoran *Scelidosaurus* for additional context. Our tibial measurement for CMNFV 22039 represents the summed length of both proximal and distal portions of the only preserved tibia; an unknown span is missing between these two pieces, so ours is a minimum estimate of tibia length. Similarly, because CMNFV 22039 lacks a metatarsal III, we measured metatarsal IV instead, which itself is missing some of the proximal portion and is always somewhat shorter than metatarsal III. Thus, our estimated length of the distal hindlimb of CMNFV 22039 represents a minimum value. We plotted hindlimb proportions in a ternary diagram.

DESCRIPTION OF CMNFV 22039

Specimen CMNFV 22039 was found loosely articulated when discovered, having the preserved elements in correct relative positions but not in contact with one another (G. Danis, pers. comm. to JCM, 2025). The specimen consists of various portions of the vertebral column and fragmentary dorsal ribs, much of the pelvic girdle, and representative portions of the hindlimb (Fig. 2). Most of the material has been taphonomically crushed or warped, but much of the original morphology is still discernible. This taphonomic alteration, combined with the liberal use of consolidant, obscures much of the original surface texture of the bones. However, some of the smaller bones, including the vertebral centra and pedal elements, do not suffer from the same degree of crushing and remain free of consolidant. The surfaces of these bones tend to be rough and grainy, marked by tiny grooves and pits (Fig. 3). A similar surface texture is seen in the long bones of bird chicks (de Rooij et al., 2023; Tumarkin-Deratzian et al., 2006).

The specimen is the smallest known pachycephalosaur for which comparable postcranial material is available (Table 1). The femur length is 91.3% that of *Wannanosaurus yansiensis*, 68.5% that of *Micropachycephalosaurus hongtuyanensis*, and 64.3% that of *Zavacephale rinpoche* Chinzorig et al., 2025, three of the smallest reported pachycephalosaurs to date (although the taxonomic status of *M. hongtuyanensis* is uncertain; Butler & Zhao, 2009; Fonseca et al., 2024).

Axial Skeleton

Vertebrae—The different regions of the axial skeleton are represented by vertebrae in various states of preservation, but we will describe only the most anatomically informative elements here. In all preserved vertebrae (11 centra and several fragmentary neural arches), the neural arches are unfused to their centra.

A single cervical vertebra is represented. The axis neural arch (Fig. 4) is low with widely spaced pedicels that would have articulated with a transversely broad centrum, which is not preserved. Similarly, transversely wide spacing of the pedicels, and consequently wide neural canal, are seen only in the cervical vertebra of *W. yansiensis* (Butler & Zhao, 2009:fig. 8A) and the atlas centrum of "*Dracorex hogwartsia*" (Bakker et al., 2006: fig. 9). The canal is much narrower in an undescribed partial skeleton of *Stygimoloch spinifer* (NSM PV 20423), but this appears to be at least partly due to transverse crushing of the element. The axis zygapophyses have eroded away in CMNFV 22039. The transverse processes are confluent with the pedicels and the diapophyseal contacts face ventrolaterally. Each transverse process is joined to the neural arch via a thin lamina of bone that ascends from the posterior edge of the transverse process to trace the ventral margin of the neural spine. The neural spine is transversely narrow and strongly inclined posteriorly so that the long axis is subhorizontal. The apical margin of the neural spine is convex in lateral profile, contrasting with the condition in *Heterodontosaurus tucki*, *Psittacosaurus sibiricus*, and *Sty. spinifer* (NSM PV 20423) in which the apex is concave (Averianov et al., 2006; Galton, 2014), yet similar to the condition in *Protoceratops andrewsi* (Brown & Schlaikjer, 1943).

Seven disarticulated centra can be attributed to the dorsal series (Fig. 5), as evidenced by the lack of parapophyseal facets. Although their precise positions within the column cannot be determined with certainty, they likely increase in size posteriorly (Table 2), as in *Hypsilophodon foxii*, *Thescelosaurus assiniboiensis*, and *Homalocephale calathocercos*. Each centrum is spool shaped and amphiplatyan to weakly amphicoelous. In each element, the floor of the neural canal is perforated by an anteroposteriorly elongate foramen (Fig. 4C), a feature also seen in *Stegoceras validum* (Gilmore, 1924) and various other neornithischian taxa (Brown et al., 2013). The lateral surfaces of the centra are similarly perforated by a still smaller foramen. The margins about the central faces are slightly crenulated, delimiting the probable attachment surfaces for intervertebral connective tissues. These crenulations are particularly well developed in *Thescelosaurus* (Brown et al., 2011), which may be one of the reasons that D. Russell referred CMNFV 22039 to that genus. There is little beyond size to distinguish the centra, although the smallest and presumably anteriormost element (Fig. 4A) is slightly more laterally compressed and less ventrally concave than the others.

There are several fragmentary neural arches attributable to the presacral series, but these are so poorly preserved as to not merit description. The single exception is a dorsal neural arch

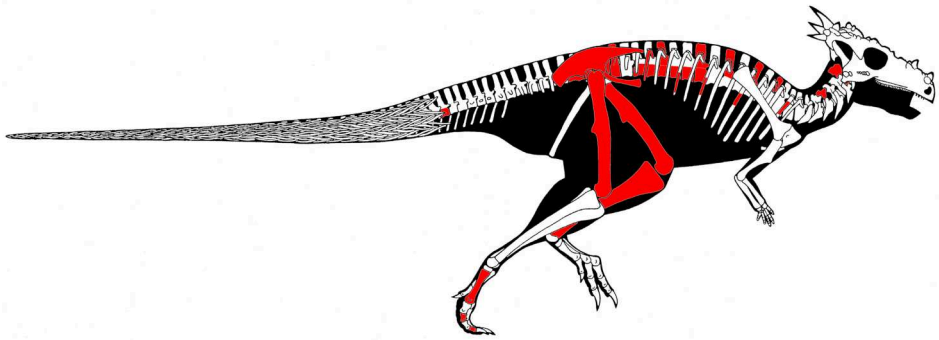

FIGURE 2. Preserved elements (in red) of juvenile Pachycephalosauria indet. (CMNFV 22039). The preserved left ischium does not show in this view. Diagram illustrates preserved elements only and does not accurately reflect the proportions of CMNFV 22039. Skeletal drawing modified after original illustrations of *Pachycephalosaurus* (postcranium) and "*Dracorex*" (cranium) by Gregory Paul. Used with permission.

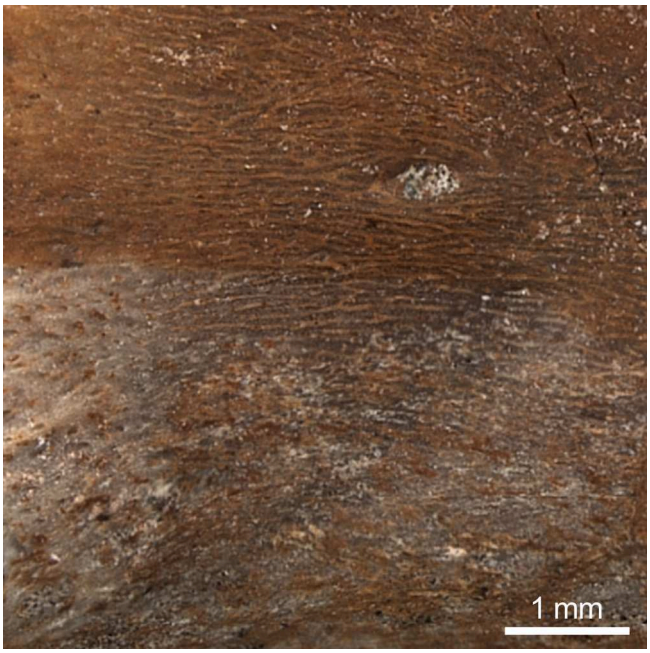

FIGURE 3. Surface texture detail of dorsal vertebra of Pachycephalosauria indet. (CMNFV 22039). Note the grainy texture and fine pitting (large opening in upper-right quadrant is a nutrient foramen).

bearing a parapophysis at the base of each transverse process (Fig. 5H, I). The neural spine is broad in the sagittal plane, the apex is somewhat expanded transversely, and the spine is inclined posteriorly, as in *H. calathocercos* (Maryańska & Osmólska, 1974). The zygapophyses bear the ridge-and-groove

FIGURE 4. Axis neural arch of juvenile Pachycephalosauria indet. (CMNFV 22039). **A**, anterior view; **B**, right lateral view.

articular surfaces characteristic of Pachycephalosauria (Maryańska et al., 2004), but their topology is shallow compared with that seen in more mature forms (Fig. 5, inset). The neural canal is much narrower than that of the axis vertebra. The horizontal attitude of both the transverse processes and the zygapophyseal faces, combined with the posterior offset of the neural spine relative to the pedicels, suggest that this is a posterior dorsal vertebra—likely the last in the series (Maryańska & Osmólska, 1974). Indeed, the neural arch affixes to the largest and presumably posteriormost of the preserved centra (Fig. 5H, I).

All three preserved sacral centra lack intercentral fusion (Fig. 6). They compare favorably with the equivalent elements illustrated for *H. calathocercos* and *Goyocephale lattimorei* (Evans et al., 2011; Maryańska & Osmólska, 1974; Perle et al., 1982). The largest of these three centra, identified as a dorsosacral ('sacral 1' of Maryańska and Osmólska, 1974), bears a crescentic union of the diapophysis-parapophysis on each posterolateral margin of the posterior intercentral face (Fig. 6A). A second preserved sacral centrum is slightly anteroposteriorly longer, but dorsoventrally shallower, in part due to taphonomic shearing of the dorsal surface (Fig. 6B). The combined apophyses are apparently situated anteriorly, and this element may have immediately succeeded the first (i.e., the first 'true' sacral). A third sacral centrum, similarly sheared, is subequal in length to the last, with a strong ventral keel (Fig. 6C). It may have occurred in the third or fourth position of the sacral series but does not clearly articulate with the preceding sacrals.

A single centrum can be positively attributed to the caudal series (Fig. 6D). It is spool shaped, and the central faces are weakly amphicoelous. It is similar in size to the anteriormost preserved dorsal vertebrae but bears ventrally placed chevron facets anteriorly and posteriorly. The relative size of the centrum and presence of chevron facets suggest that the element originally occurred near the middle of the caudal series. The anterior and posterior chevron facets are linked by a pair of weak longitudinal ridges, as in *H. calathocercos* (Maryańska & Osmólska, 1974).

Dorsal ribs—Several fragmentary dorsal ribs were recovered with the specimen. These generally lack both articular and distal ends, and their fragmentary nature makes them difficult to place within the axial skeleton. One proximal rib fragment has a poorly developed tuberculum and resembles a putative mid-dorsal rib of *Ste. validum* (Gilmore, 1924). Some of the straighter rib fragments may come from further anteriorly in the dorsal series. A single preserved sacral rib is distinctly robust and hourglass-shaped. The distal end fits snugly against the medial surface of the right ilium, above the ischial peduncle, suggesting that it is sacral rib 5 (Maryańska et al., 2004). A final rib is gently curved, with an abbreviated capitulum and tuberculum, and may represent a caudal rib (Maryańska *et al*., 2004).

Pelvic Girdle

The pelvic girdle and sacral elements (Fig. 7) are complete enough to allow, with mirroring, a reconstruction of the total breadth of the hips, which are approximately 8 cm across the posterior ends of the ilia (Fig. 7B).

Ilium—A single right ilium is preserved (Fig. 8). It is weakly sigmoidal in dorsal view, as in all pachycephalosaurs and *T. assiniboiensis* (Brown et al., 2011; Evans et al., 2013b; Maryańska et al., 2004; Williamson & Brusatte, 2016); by contrast, the ilia of *Stenopelix valdensis* and *Psittacosaurus mongoliensis* Osborn, 1923 are uniformly bowed laterally when viewed dorsally (Butler & Sullivan, 2009; Maryańska et al., 2004; Sereno, 1987; Sereno et al., 1988; Sues & Galton, 1982). Mediolateral crushing of the ilium of CMNFV 22039 likely reduced the

TABLE 1. Comparative postcranial measurements of pachycephalosaurs (in mm). Asterisk (*) denotes minimal estimate influenced by breakage. Note that the pachycephalosaurian status of *Micropachycephalosaurus hongtuyanensis* is uncertain (Butler & Zhao, 2009).

Taxon	Specimen	Ilium length	Femur length	Tibia length	Source
Pachycephalosauria indet.	CMNFV 22039	107	85	77*	This study
Wannanosaurus yansiensis	IVPP V 4447	?	93	86	Butler & Zhao, 2009
Micropachycephalosaurus hongtuyanensis	IVPP V 5542	?	124	?	Butler & Zhao, 2009
Prenocephale prenes	MPC-D 100/1204	226	222	?	Maryańska & Osmólska, 1974
Homalocephale colathocercos	MPC-D 100/1201	230	218	?	Maryańska & Osmólska, 1974
Goyocephale lattimorei	MPC-D 100/1501	230	?	?	Perle et al., 1982
Stegoceras validum	UALVP 2 (cast at CMN)	282	222	220	This study
Stygimoloch spinifer	NSM PV 20423 (cast at CMN)	370	440	381	This study

sigmoidal curvature by reducing the lateral and medial deviations of the pre- and postacetabular processes, respectively.

As preserved, the preacetabular process deviates laterally from the long axis of the element at an angle of ~12°. It also curves ventrally and becomes dorsoventrally taller towards its anterior end. The preacetabular process is ~50% longer than the postacetabular process and is mediolaterally narrow. By contrast, the pre- and postacetabular processes are subequal in length in pachycephalosaurids such as *Steg. validum*, *H. calathocercos*, *G. lattimorei*, *Prenocephale prenes*, and *Sty. spinifer* (Gilmore, 1924; JCM, pers. obs., 2025; Maryańska & Osmólska, 1974; Perle et al., 1982).

The main body of the ilium, between the pre- and postacetabular processes, is weakly concave on both medial and lateral surfaces. A deep, oval depression occurs on the medial face, extending onto the ischial peduncle (Fig. 8D), likely for the attachment of the fourth or fifth sacral ribs (Maryańska et al., 2004). The acetabular portion of the ilium is circumscribed by the smaller pubic and larger ischial peduncles. The pubic peduncle projects anteroventrally, becoming wider anteriorly, as in *Steg. validum* and *Thescelosaurus neglectus* (Gilmore, 1915, 1924). In *Ps. mongoliensis* and *Sten. valdensis*, the pubic peduncle projects more strongly ventrally than anteriorly (Sereno, 1987; Sues & Galton, 1982). The ischial peduncle is ~70% wider than the pubic peduncle and more bulbous. The ilium possesses the characteristic medial flange of pachycephalosaurs (except *Zavacephale rinpoche*) immediately posterodorsal to the acetabulum (Fig. 8B; Chinzorig et al., 2025; Gilmore, 1924; Perle et al., 1982; Sues & Galton, 1982; Sereno, 1987). It projects from the dorsal margin of the ilium at an angle of ~70° from the horizontal. There is some taphonomic crushing about the base of the flange, and it is possible that the projection angle was originally closer to 40°, as in *Steg. validum* (UALVP 2). The medial flange of all other known pachycephalosaurs (e.g., *H. calathocercos*, *Pr. prenes*), except *Z. rinpoche*, projects strongly horizontally (Chinzorig et al., 2025, Maryańska et al., 2004; Perle et al., 1982; Williamson & Brusatte, 2016).

The postacetabular process of the ilium deviates medially at an angle of ~17° from the long axis of the element. The process exhibits the typical mediolateral curvature and subrectangular shape of other pachycephalosaurids (Maryańska et al., 2004; Perle et al., 1982). Some pachycephalosaurs, including *H. calathocercos* and *Sty. spinifer*, possess a postacetabular process that is greatly curved ventrally (JCM, pers. obs., 2025; Perle et al., 1982). CMNFV 22039 displays the condition observed in other pachycephalosaurs, such as *Steg. validum* and *G. lattimorei*, where the postacetabular process exhibits little to no ventral curvature (Perle et al., 1982). Measurements of the pelvic elements are given in Table 3.

Pubis—The right pubis (Fig. 9) is reduced and gracile compared with all consulted outgroup taxa (Brown, 2009; Brown et al., 2011; Dieudonné et al., 2021; Gilmore, 1915; Sereno, 1987; Sereno et al., 1988), and the posteriormost tip is missing. The rod-like prepubic process is elongate, though it does not extend anteriorly as far as the preacetabular process of the ilium in *T. neglectus* (Gilmore, 1915) and *H. calathocercos* (Maryańska & Osmólska, 1974). In CMNFV 22039, the prepubic process is straight. By comparison, the prepubic process of *H. calathocercos* (MPC-D 100/1201) is curved laterally. The prepubic process is slightly dorsoventrally expanded in CMNFV 22039; it narrows where it joins the main body of the pubis.

The iliac and ischial peduncles of the pubis are not as distinct as they are in most other ornithischians (e.g., hadrosaurids, ceratopsids). Instead, these peduncles are little more than flattened contacts, set off from one another by approximately 45°. The iliac contact faces dorsally, whereas the ischial contact faces ventrolaterally. Such an arrangement almost precludes the pubis from contributing to the rim of the acetabulum, which is typical of pachycephalosaurs (Maryańska et al., 2004).

TABLE 2. Centrum measurements (in mm) of juvenile Pachycephalosauridae indet. (CMNFV 22039). Asterisk (*) denotes incomplete measurement. Dorsals are lettered in ascending order of size to reflect positional uncertainty within the series.

Centrum	Height	Width	Length
Dorsal A	7.4	8.3	9.7
Dorsal B	7.6	8.5	9.7
Dorsal C	8.1	8.9	10.1
Dorsal D	9.5	9.6	10
Dorsal E	8.7	9.5	10.4
Dorsal F	9.1	9.2	10.9
Dorsal G	10.9	11.6	12.2
Dorsosacral	11.1	13.7	13.6
Sacral 1	10.9	12.6	16.3*
Sacral 3 or 4	?	?	19.8*
Middle caudal	7.7	8.7	9.1

TABLE 3. Maximum length measurements (in mm) of pelvic girdle elements for juvenile Pachycephalosauridae indet. (CMNFV 22039).

Element	Length
Right ilium (measured from the anterior tip of the preacetabular process to the posterior tip of the postacetabular process)	107.0
Ischium (measured from the pubic peduncle to the distal end of the shaft)	98.5
Pubis (measured from the posterior tip of the true pubis to the anterior tip of the prepubic process)	46.0

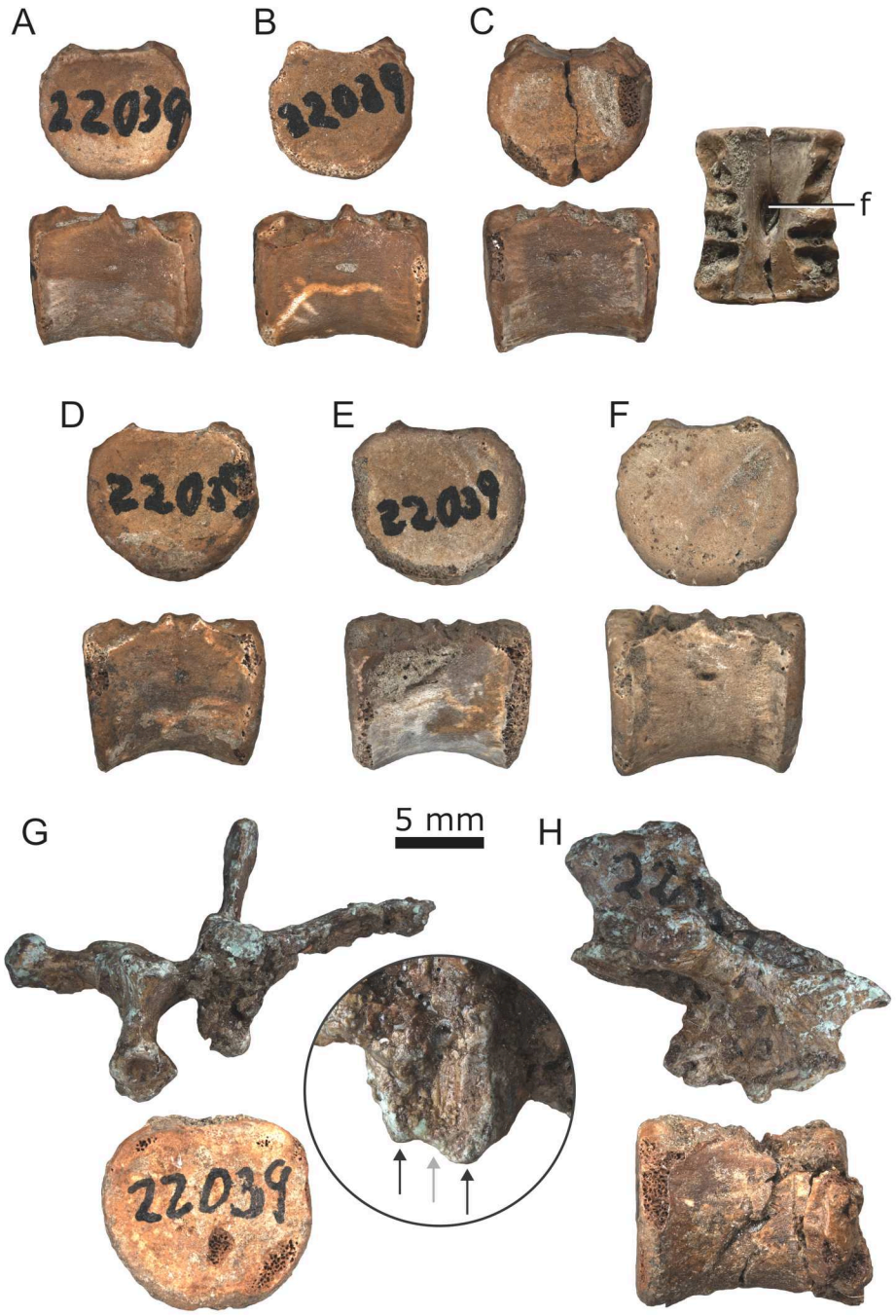

FIGURE 5. Dorsal vertebrae of juvenile Pachycephalosauria indet. (CMNFV 22039). **A–F**, isolated centra in anterior (top) and lateral (bottom) views (**C** also shows dorsal view at right, showing foramen (**f**) in floor of neural canal); **G**, probable posteriormost dorsal vertebra in anterior view; **H**, same dorsal vertebra in right lateral view. Inset depicts postzygapophysis of dorsal neural arch in **G** and **H**, with arrows showing ridge- (black) and- groove (gray) system.

Ischium—The rod-like left ischium (Fig. 10) is proximally expanded to form the pubic and iliac peduncles. The slender pubic peduncle is anteriorly elongate and articulates with the pubis. The iliac peduncle is anteroposteriorly broad with a concave dorsal articulation to receive the corresponding peduncle of the ilium. The ischium possesses no obturator process, as in all marginocephalians (Butler & Sullivan, 2009). The shaft of the ischium is long, uniformly slender, gently bowed posteriorly, and slightly curved medially. This form is similar across Pachycephalosauria. The morphology differs from that of the outgroup taxon *Sten. valdensis*, where the shaft is notably kinked (Sues & Galton, 1982), and *H. tucki*, where the shaft is straight (Dieudonné et al., 2021).

Hindlimb

Although neither hindlimb is complete, the gross anatomy can still be reconstructed from the available material (see also 'Analysis of Hindlimb Proportions' below). The condyles of the long bones of the hindlimbs are well formed, contrasting with the condition of presumably altricial juvenile dinosaurs, wherein the articular condyles are poorly developed (e.g.,

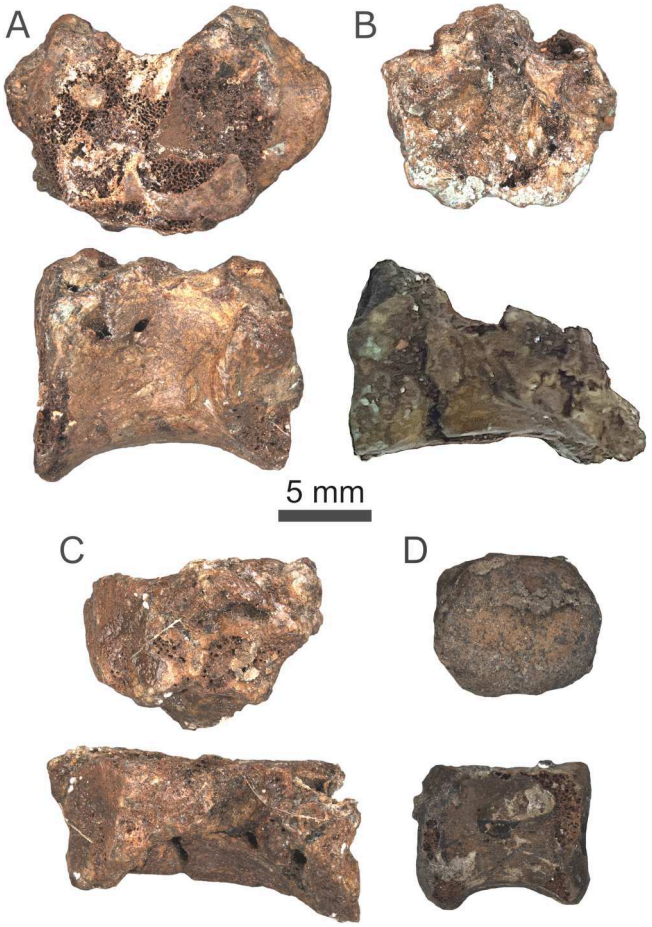

FIGURE 6. Sacral and caudal vertebrae of juvenile Pachycephalosauria indet. (CMNFV 22039). **A**, dorsosacral centrum in anterior (top) and lateral (bottom) views; **B**, sacral centrum 1 in anterior (top) and lateral (bottom) views; **C**, third or fourth sacral centrum in posterior (top) and lateral (bottom) views; **D**, middle caudal vertebra in anterior (top) and left lateral (bottom) views.

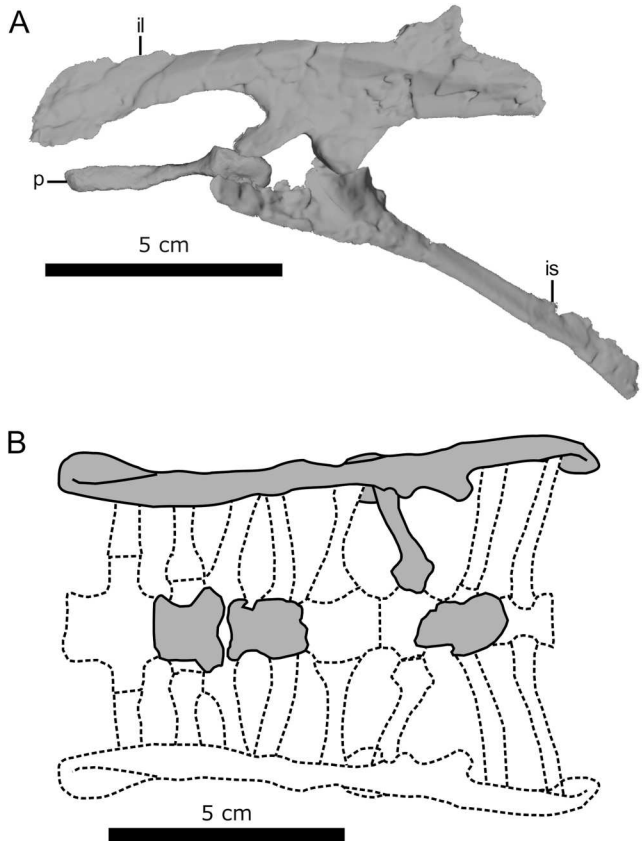

FIGURE 7. Reconstructed pelvis of juvenile Pachycephalosauria indet. (CMNFV 22039). **A**, pelvis in left lateral view (ilium and pubis mirrored). **B**, pelvis in dorsal view, anterior to the left (dotted lines denote reconstruction). **Abbreviations: il**, ilium; **is**, ischium; **p**, pubis.

Chure et al., 1994; Horner & Weishampel, 1988; Jacobs et al., 1994).

Femur—Both femora are present (Fig. 11), but each suffers from various degrees of taphonomic distortion. The distal condyles of the right femur, while preserved, have broken away from the remainder of the element. The following description draws from the best-preserved aspects of each element.

The femoral head is well offset from the shaft and projects dorsomedially towards the acetabulum. It is moderately anteroposteriorly compressed, which is common among pachycephalosaurs (Maryańska et al., 2004). The greater trochanter is well developed and lies posterolateral to the femoral head. It forms a large, rectangular expansion that is separated from the femoral head by a deep cranial intertrochanteric groove. The ridge-like lesser trochanter extends down the diaphysis approximately as far as the neck of the femoral head.

The diaphysis is badly crushed in each element, but the left element shows that the femur was bowed laterally. The fourth trochanter occurs a little less than halfway down the length of the diaphysis, on the posterior surface. This positioning of the fourth trochanter is similar to *H. calathocercos* (MPC-D 100/1201), *Pr. prenes* (MPC-D 100/1204), and *Z. rinpoche* (MPC-D 100/1209). In *Sty. spinifer* (NSM PV 20423) and *Steg. validum* (UALVP 2), it is located nearer the midpoint of the diaphysis (Gilmore, 1924; Maryańska et al., 2004; Perle et al., 1982), and it is positioned directly at the midpoint in *W. yansiensis* (Butler & Zhao, 2009). The fourth trochanters of *T. assiniboiensis*, *Ps. mongoliensis*, and *Sten. valdensis* are also proximally positioned (Brown, 2009; Brown et al., 2011; Gilmore, 1915; Sereno, 1987;

TABLE 4. Limb bone measurements (in mm) of CMNFV 22039 (* indicates measurements that are likely altered by taphonomic deformation).

Element	Proximodistal length	Midshaft mediolateral diameter	Midshaft anteroposterior diameter	Midshaft circumference
Left femur	84.5	6.5	13.0	35.1
Right femur	100.5*	12.0	6.4	34.5
Left tibia	?	7.7	?	?
Left fibula	?	4.2	?	?

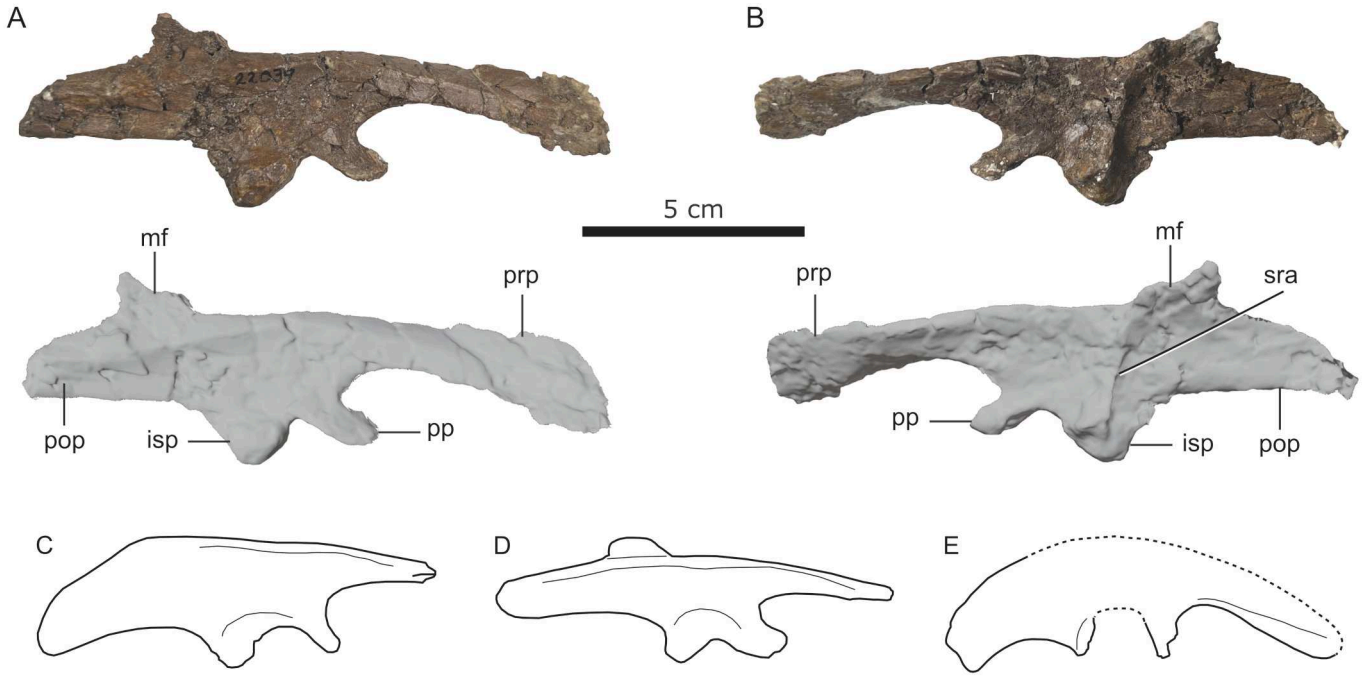

FIGURE 8. Right ilium of juvenile Pachycephalosauria indet. (CMNFV 22039) and comparisons. **A**, lateral view; **B**, medial view. **C**, right ilium of *Homalocephale calathocercos* (MPC-D 100/1201) in lateral view; **D**, right ilium of *Stegoceras validum* (UALVP 2) in lateral view; **E**, left ilium (reversed for comparison) of *Stygimoloch spinifer* (NSM PV 20423) in lateral view. **Abbreviations**: **isp**, ischial peduncle; **mf**, medial flange; **pop**, postacetabular process; **pp**, pubic peduncle; **prp**, preacetabular process; **sra**, sacral rib attachment.

Sereno et al., 1988). The fourth trochanter of CMNFV 22039 is also weakly pendant, although the tip is broken in each counterpart (Fig. 12). This condition is not observed in most other pachycephalosaurs, which generally display a non-pendant fourth trochanter, except *Pr. prenes* (MPC-D 100/1204). By comparison, the fourth trochanters of the outgroup taxa *T. assiniboiensis*, *Ps. mongoliensis*, and *Sten. valdensis* are all strongly pendant (Brown, 2009; Brown et al., 2011; Gilmore, 1915; Sereno, 1987; Sereno et al., 1988).

The distal end of the femur expands to form prominent lateral and medial condyles, the latter being slightly wider transversely than the former. The condyles protrude strongly posteriorly

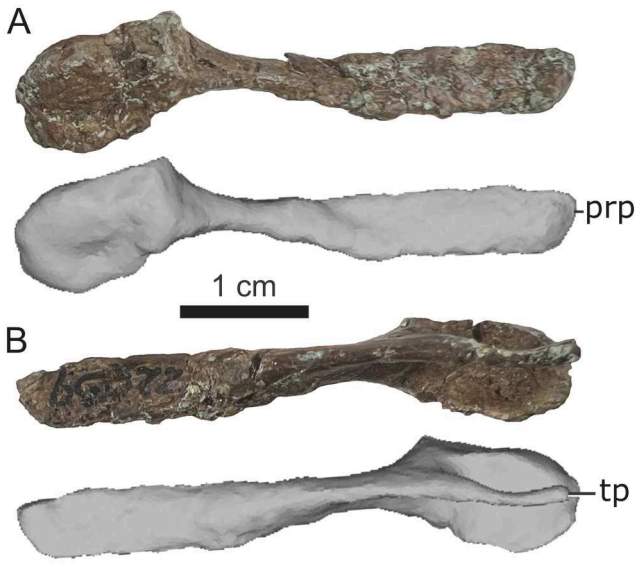

FIGURE 9. Right pubis of juvenile Pachycephalosauria indet. (CMNFV 22039). **A**, lateral view; **B**, medial view. **Abbreviations**: **prp**, prepubic process; **tp**, 'true' pubis.

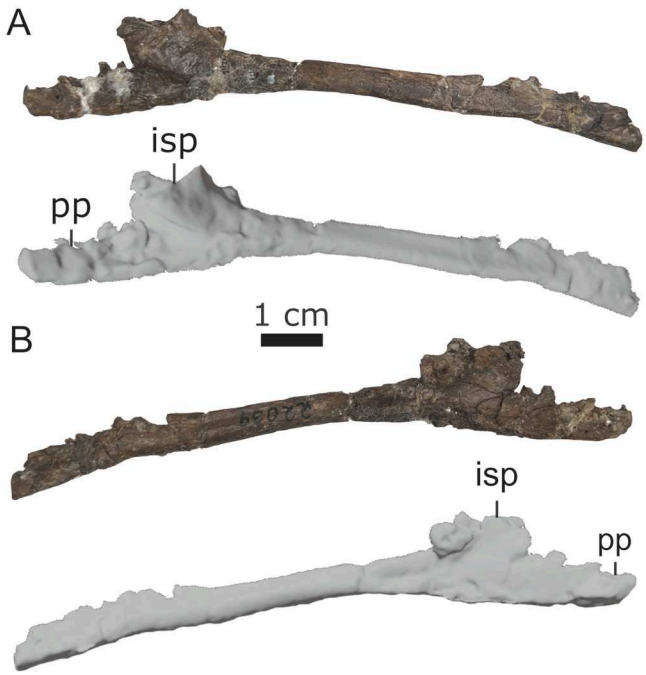

FIGURE 10. Left ischium of juvenile Pachycephalosauria indet. (CMNFV 22039). **A**, lateral view; **B**, medial view. **Abbreviations**: **isp**, ischial peduncle; **pp**, pubic peduncle.

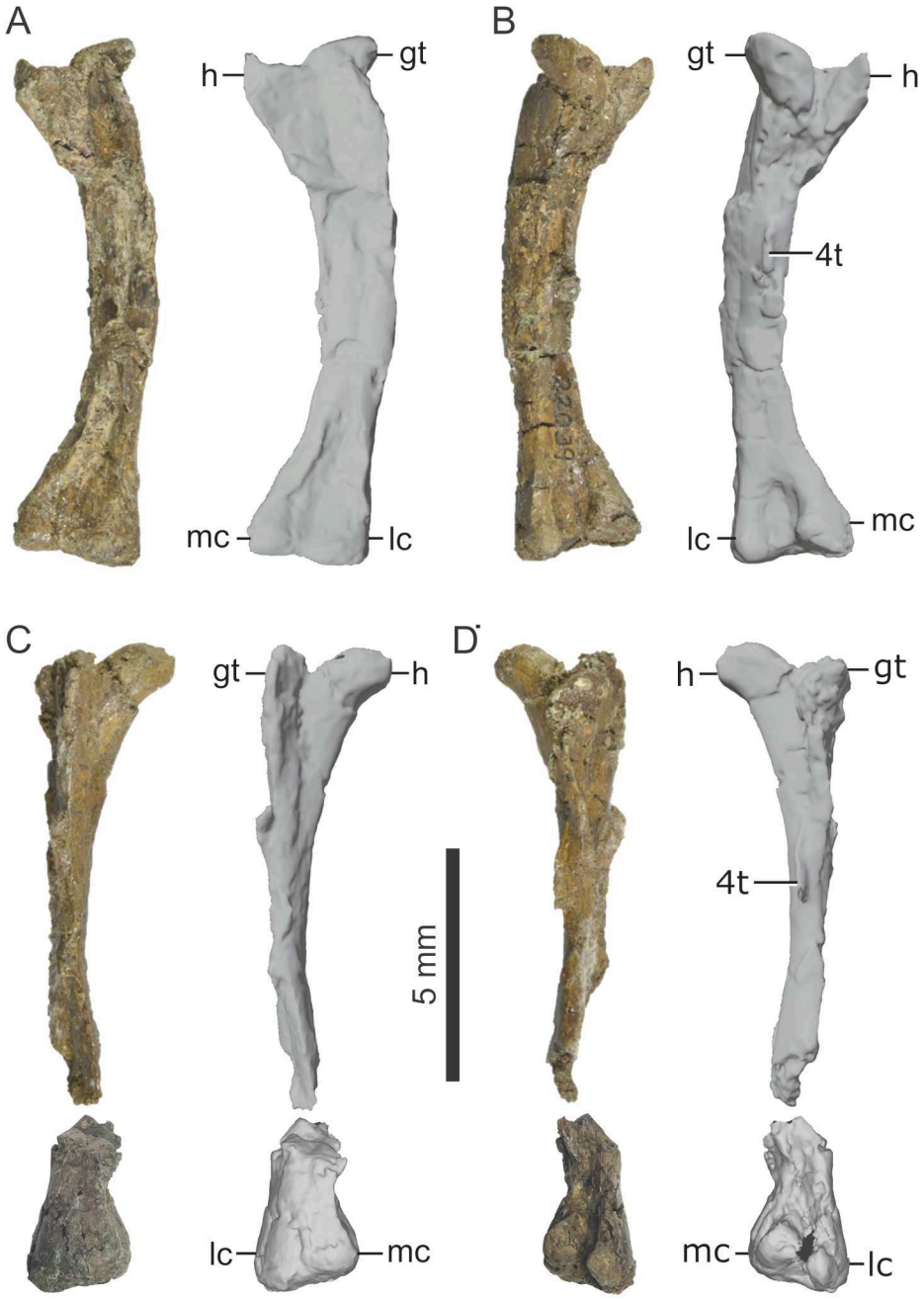

FIGURE 11. Femora of juvenile Pachycephalosauria indet. (CMNFV 22039). Left femur in anterior, **A**, and posterior, **B**, views; right femur in anterior, **C**, and posterior, **D**, views. **Abbreviations**: **4t**, fourth trochanter; **gt**, greater trochanter; **h**, femoral head, **lc**, lateral condyle, **mc**, medial condyle.

and are separated from each other by a deep, rectangular groove. Measurements of the femora and other limb elements are given in Table 4.

Tibia—Only the left tibia is preserved. It articulates proximally with the corresponding fibula; the elements remain cemented together postdepositionally (Fig. 13). The tibia is a dorsoventrally elongate, straight element with a slender diaphysis and well-developed proximal and distal expansions. There is a break in the tibia separating the distal third of the diaphysis from the distal condyles; the intervening portion is missing. The proximal articular surface of the tibia is slightly concave and is separated by a shallow groove into a lateral and medial condyle of equal size. This groove extends distally along the posterior surface of the element, gradually shallowing until it disappears where the proximal expansion merges into the diaphysis. The cnemial crest is subrectangular in profile and extends over the anteromedial surface of the fibula. It appears to have been crushed in this direction. The proximal expansion gradually and uniformly thins distally towards the diaphysis. Where the proximal expansion and diaphysis meet, a significant lateral portion of the diaphysis has broken away, leaving a large cavity that encompasses approximately one third of the presumed diaphyseal length as it extends distally. The diaphysis gradually thins distally until the break. The proximal expansion of the tibia is slightly larger than its distal expansion, but this is likely exaggerated by lateral compression of the cnemial crest. The distal

FIGURE 12. Pendant fourth trochanter of juvenile Pachycephalosauria indet. (CMNFV 22039) (right) compared with femoral outlines (not to scale) of *Thescelosaurus assiniboiensis* (left) and *Stegoceras validum* (middle) all in lateral view. **Abbreviation**: **4t**, fourth trochanter.

medial condyle is slightly larger than the lateral condyle. They are separated by a shallow concavity along the distal and anterior faces. In other pachycephalosaurids (e.g., *Steg. validum*) the lateral distal condyle is more prominent than the medial (Maryańska et al., 2004). Both condyles are subrectangular, and their distal articular surfaces are shallowly concave.

Fibula—Only the proximal half of the left fibula of CMNFV 22039 is preserved (Fig. 13). It is more gracile than the tibia and is slightly curved medially. The proximal end of the element is weakly expanded and gradually thins distally. The entire element is mediolaterally compressed and slightly concave on its medial surface to accept the diaphysis of the tibia. This overall morphology is consistent with all other pachycephalosaurs and the examined outgroup taxa (Brown et al., 2011; Butler & Sullivan, 2009; Gilmore, 1915, 1924; Maryańska et al., 2004; Perle et al., 1982; Sereno, 1987; Sereno et al., 1988; Sues & Galton, 1982).

Pes

Metatarsals—The metatarsals associated with the specimen are fragmentary; the most complete is a right metatarsal IV (Fig. 14A). This element is missing the proximal end and is badly crushed, but the distal end has a triangular articular face, as in *Steg. validum*. The medial surface is flat along the contact with metatarsal III. A fragmentary, probable right metatarsal III is represented by proximal and distal fragments (Fig. 14A). The proximal articular face is ovoid, and the shaft is transversely narrow to receive the adpressed metatarsals. The distal end is transversely wide and forms a distinctive trochlea, with subequally sized condyles.

Phalanges—Two pedal phalanges are preserved, one being 25% longer than the other (Fig. 14B). These bear the expected trochleated distal articular surfaces and shallow ligamentous pits distally. The phalanges are asymmetric and so likely pertain to one of the abaxial digits—likely, digit IV.

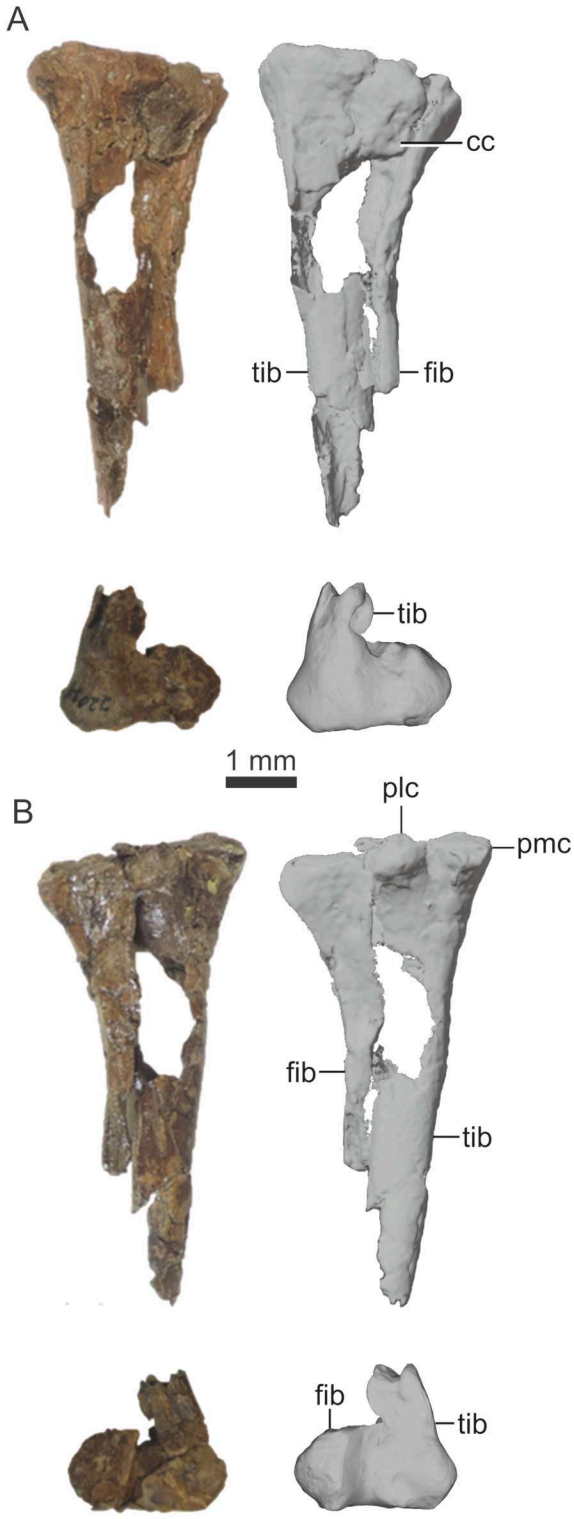

FIGURE 13. Left tibia and fibula of juvenile Pachycephalosauria indet. (CMNFV 22039). **A**, anterior view; **B**, posterior view. **Abbreviations**: **cc**, cnemial crest; **fib**, fibula; **plc**, proximal lateral condyle; **pmc**, proximal medial condyle; **tib**, tibia.

They closely resemble the phalanges illustrated for *G. lattimorei* (Perle et al., 1982) and *Z. rinpoche* (Chinzorig et al., 2025). Their small size suggests they are located distally on the digits.

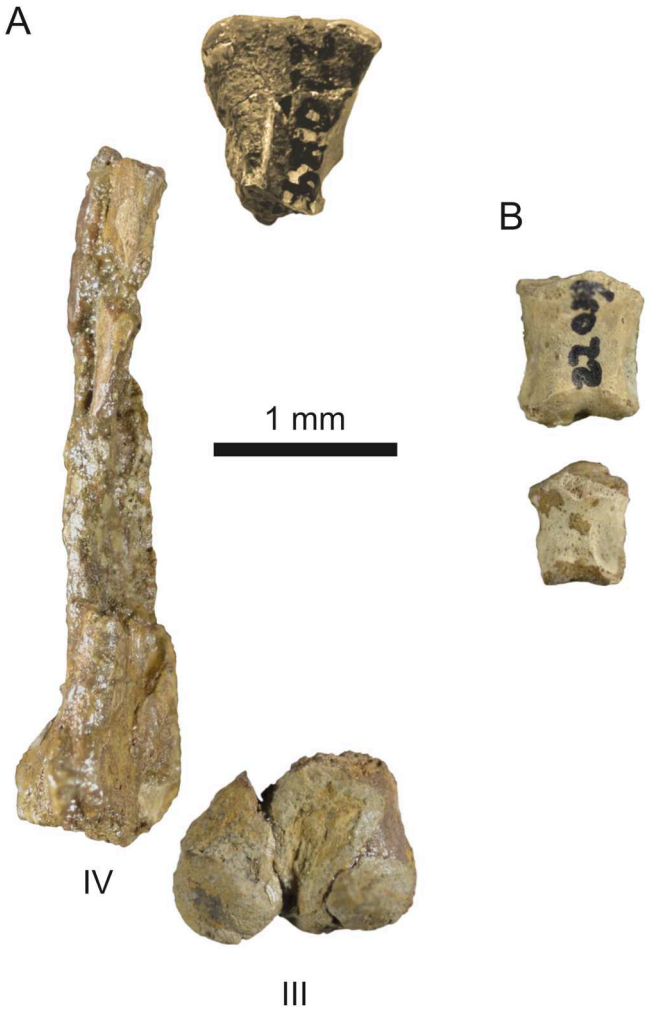

FIGURE 14. Pedal elements of juvenile Pachycephalosauria indet. (CMNFV 22039). **A**, preserved ?right metatarsals III and IV in anterior view; **B**, preserved pedal phalanges in dorsal view.

HISTOLOGICAL ANALYSIS

The cortex of the tibia and fibula consists entirely of highly vascularized woven bone, which appears isotropic under cross-polarized light. Although all woven bone is disorganized (Francillon-Vieillot et al., 1990; Lamm & Werning, 2013), there is a clear distinction between levels of vascularization and organization evident in the tibia of CMNFV 22039 (Fig. 15). The bone adjacent to the marrow cavity in the inner cortex is highly vascular and reticular in organization, abruptly transitioning to a more plexiform-style of organization near the mid-cortex. A similar transition occurs in the fibula of CMNFV 22039; however, the abrupt change in organization and vascularity is less pronounced (Fig. 15). This boundary may represent a hatching line, marking the transition from prenatal to postnatal bone (Curry Rogers et al., 2016). Additionally, vascular canals open to the bone surface, indicating rapid and active growth (Redelstorff & Sander, 2009). In the absence of obvious, longitudinally oriented osteons, sensu Lamm and Werning (2013), the bone cannot be described as fibrolamellar. There is no evidence for secondary remodeling (e.g., secondary osteons) or lines of arrested growth (Francillon-Vieillot et al., 1990; Lamm & Werning, 2013).

PHYLOGENETIC ANALYSIS

Our analysis using equal character weighting recovered 153,913 most parsimonious trees (Supplementary File 4) of 146 steps each (consistency index [CI] = 0.76, retention index [RI] = 0.79). The strict consensus tree (Fig. 16A) is very poorly resolved, with the ceratopsian *Yinlong* and the pachycephalosaurs *Wannanosaurus* and *Zavacephale* recovered as successively more derived than the outgroup, *Psittacosaurus*. All pachycephalosaurs more derived than *Zavacephale* collapse into a polytomy, with CMNFV 22039 among them.

Implied weighting recovers 2335 most parsimonious trees (Supplementary File 5), each with a score of 2.66 and a length of 146 steps (CI = 0.76, RI = 0.79). Resolution within the strict consensus tree is only marginally improved, with *Sinocephale* recovered as the next most derived pachycephalosaur (Fig. 16A). CMNFV 22039 is again recovered in a polytomy with the remaining pachycephalosaurs. Bootstrap values supporting the relationships of basally-branching pachycephalosaurs and the immediate outgroups are strong (≥88%); however, support for relationships within Pachycephalosauridae (sensu Madzia et al., 2021) is consistently <50% (Fig. 16A).

We made a further attempt to improve phylogenetic resolution by pruning unstable taxa from the above implied weighting analysis using the Trees→Comparisons→Pruned Trees command in TNT, allowing for the pruning of up to 10 taxa and otherwise using default settings. The following seven unstable taxa were identified: *Acrotholus*, *Alaskacephale*, *Amtocephale*, *Platytholus*, *Sphaerotholus edmontonensis*, *Sphaerotholus goodwini*, and *Sphaerotholus lyonsi*. Pruning these taxa yields a highly resolved reduced strict consensus tree (Fig. 16B; score = 2.33, length = 181 steps, CI = 0.63, RI = 0.58) (Supplementary File 6), which is consistent with the four reduced strict consensus trees produced by Chinzorig et al. (2025:extended data fig. 7i–l). However, unlike that study, our analysis does not recover *Tylocephale* or *Pachycephalosaurus* as unstable taxa, so these were not pruned from the reduced strict consensus tree. *Tylocephale* is instead recovered as the most basally-branching member of Pachycephalosaurinae (sensu Madzia et al., 2021), and *Pachycephalosaurus* occurs in a polytomy with the clades (*Sp. triregnum*, *Sp. buchholtzae*) and (*Goyocephale*, *Homalocephale*). CMNFV 22039 is the sister to *Prenocephale*, both of which are united by a single unambiguous synapomorphy (Char. 85[1]: weakly pendant fourth trochanter of the femur).

ANALYSIS OF HINDLIMB PROPORTIONS

Ornithischians vary widely in their hindlimb proportions (Fig. 17), especially in the contribution of the femur to limb length. At one end of the spectrum, heterodontosaurids are characterized by relatively short femora (30–35% of hindlimb length) and correspondingly long tibiae and metatarsals, typical of cursorial forms. At the other end of the spectrum, the bipedal thescelosaurids, large ornithopods, and the quadrupedal *Scelidosaurus* have proportionately long femora (40–50% of hindlimb length) and short distal hindlimb elements, suggesting a more ponderous gait. Basally-branching ceratopsians, basally-branching ornithischians, and small ornithopods span these extremes. The early pachycephalosaur *Zavacephale* plots towards the heterodontosaurids, among the basally-branching ornithischians. The more derived *Stegoceras* plots with the large ornithopods and thescelosaurids, having proportionally long femora. CMNFV 22039 has hindlimb proportions somewhere between those of *Zavacephale* and *Stegoceras*, somewhat closer to the latter than the former (Fig. 17). However, given that the lengths of the tibia and metatarsal III of CMNFV 22039 are minimum estimates, the original limb proportions of the animal may have more closely resembled those of *Zavacephale*.

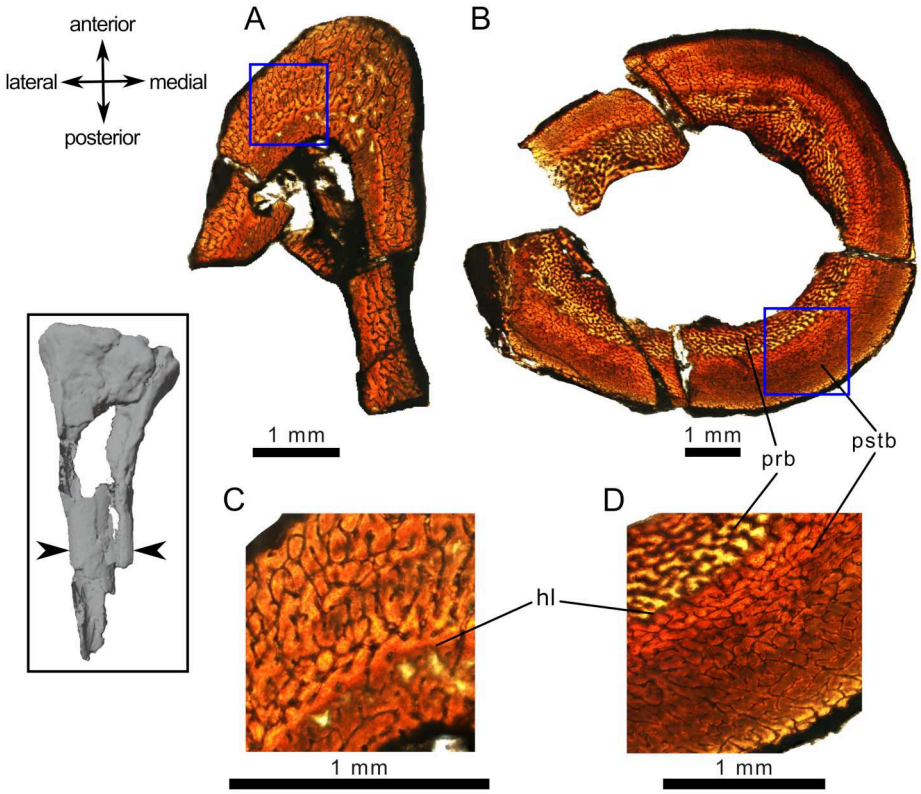

FIGURE 15. Mid-diaphyseal transverse sections of the fibula and tibia of juvenile Pachycephalosauria indet. (CMNFV 22039) under normal light. **A**, fibula under 4× magnification; **B**, tibia under 4× magnification; **C**, fibula under 50× magnification; **D**, tibia under 50× magnification. Blue boxes indicate areas of higher magnification in **C** and **D**. Inset shows line of transverse section (arrowheads). **Abbreviations**: **hl**, hatching line; **prb**, prenatal bone, **pstb**, postnatal bone.

DISCUSSION

Estimated Age-at-death of CMNFV 22039

The skeleton of CMNFV 22039 is clearly that of an early-stage juvenile (sensu Hone et al., 2016), supported by multiple lines of evidence. The right femur is just 45% as long as that of the more skeletally mature UALVP 2, *Stegoceras validum* (Gilmore, 1924). The reconstructed skeleton of UALVP 2 is approximately 2 m long; assuming isometric scaling, the skeleton of CMNFV 22039 would have been only ~90 cm long. Application of developmental mass extrapolation in the R package MASSTIMATE (Campione, 2020), using UALVP 2 as a near-adult proxy and assuming isometry, yields an estimated body mass of 2.2 kg for CMNFV 22039, based on its minimum femoral shaft circumference. Specimen CMNFV 22039 is thus an extremely small pachycephalosaur. Larger pachycephalosaurs, such as *P. wyomingensis*, are estimated to have been 370 kg as adults, while smaller members, such as *Steg. validum* and *Zavacephale rinpoche*, may have weighed up to 17 kg and 6 kg, respectively (Chinzorig et al., 2025). The lack of sacral and neurocentral fusion, otherwise present in most adult reptiles, and the grainy and porous bone surface texture also evince skeletal immaturity (Brochu, 1996; de Rooij et al., 2023; Evans et al. 2011; Griffin et al., 2021; Hoffman & Sander, 2014; Irmis, 2007; Tumarkin-Deratzian et al., 2006).

The tibial and fibular cortices of CMNFV 22039 are composed entirely of highly vascularized woven bone (Fig. 15), which is the fastest deposited bone tissue type found only in fast-growing, immature animals and fracture calluses (Castanet et al., 2000; de Margerie et al., 2002; Francillon-Vieillot et al., 1990; Lamm & Werning, 2013; Prieto-Márquez et al., 2016a; Prieto-Márquez et al., 2016b). Comparing the tibial and fibular cortices of CMNFV 22039 to mid-diaphyseal transverse sections of the femora of embryonic dinosaurian specimens (*Orodromeus makelai* Horner & Weishampel, 1988, *Troodon formosus* Leidy, 1856, *Maiasaura peeblesorum* Horner & Makela, 1979, *Hypacrosaurus stebingeri* Horner & Currie, 1994) (Horner et al., 2001) reveals distinct similarities. In particular, the inner disorganized cortex of CMNFV 22039 is remarkably similar to embryonic dinosaurian bone in level of organization and vascularity. This may suggest that the distinct boundary between the inner and mid-cortex in the tibia and fibula of CMNFV 22039 may represent a hatching line. Secondary remodeling typical of skeletally maturing individuals (Castanet et al., 2000; de Margerie et al., 2002; Francillon-Vieillot et al., 1990; Lamm & Werning, 2013; Prieto-Márquez et al., 2016a; Prieto-Márquez et al., 2016b) is lacking, as are cyclical growth marks (e.g., lines of arrested growth), indicating that this individual likely died before it had reached 1 year of age.

Taxonomic Identity of CMNFV 22039

Contrary to the initial finding of Russell and Manabe (2002), CMNFV 22039 does not pertain to *Thescelosaurus*; it is attributable to Pachycephalosauria (Fig. 18), based on the presence of (1) a double ridge-and-groove articulation on the pre- and postzygapophyses of the dorsal neural arches, (2) a medial flange on the postacetabular process of the ilium, and (3) a highly reduced pubis that contributes only minimally to the acetabulum margin (Maryańska et al., 2004). The variable presence of these features in the immature pachycephalosaurs *H. calathocercos* (MPC-D 100/1201) and *Z. rinpoche* (MPC-D 100/1209) further

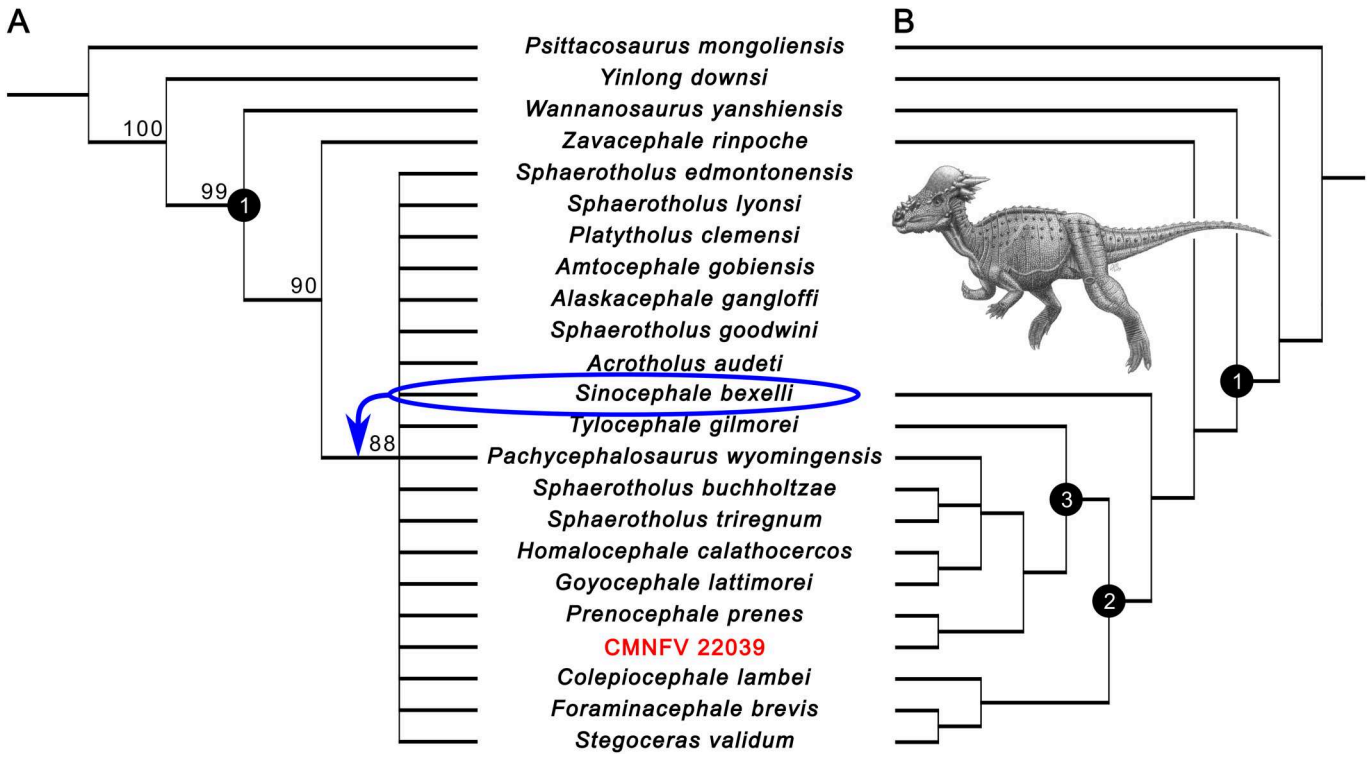

FIGURE 16. Results of cladistic parsimony analysis. **A**, strict consensus tree using equal character weighting. *Sinocephale bexelli* (circled) is resolved from the large polytomy using implied weighting (k = 12). **B**, reduced strict consensus tree following the deletion of seven unstable taxa. Node 1 = Pachycephalosauria, node 2 = Pachycephalosauridae, node 3 = Pachycephalosaurinae. Numbers above nodes are absolute bootstrap frequencies (only values >50% reported).

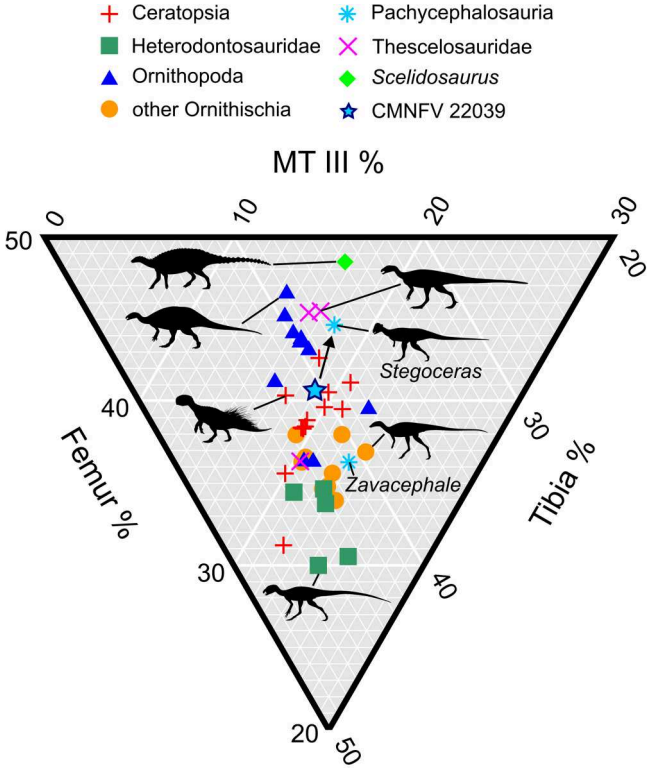

FIGURE 17. Ternary diagram of ornithischian hindlimb proportions. The arrow shows the approximate presumed ontogenetic trajectory of CMNFV 22039. **Abbreviation**: **MT III**, metatarsal III. Silhouettes from https://www.phylopic.org/ (contributors: Matt Dempsey, Scott Hartman, Jaime Headden).

substantiates the diagnosis of CMNFV 22039 as a member of Pachycephalosauria, as it shows that these diagnostic characters are present in other juveniles, even if they are of an older life stage (Chinzorig et al., 2025; Evans et al., 2011; Maryańska & Osmólska, 1974). Characters deemed diagnostic of *Thescelosaurus* are entirely isolated to the cranium (Boyd et al., 2009), which is absent in CMNFV 22039. Assignment of CMNFV 22039 to *Thescelosaurus* is therefore unsubstantiated. The presence of skeletal characters diagnostic at the infraorder level in such an immature animal is important, because it provides some reason to be optimistic about our ability to identify specimens from across the entire pachycephalosaur growth trajectory, even in the absence of characteristic cranial material.

On the other hand, the lack of cranial material makes confident identification of CMNFV 22039 beyond Pachycephalosauria indet. nearly impossible. Although our cladistic analysis recovers the specimen as a pachycephalosaurine pachycephalosaurid, the traits diagnosing these clades relate almost entirely to the skull (Maryańska et al., 2004; Sullivan, 2006) and are therefore ambiguous synapomorphies in our recovered topologies. Conversely, most other pachycephalosaurid taxa lack postcranial data altogether (Evans et al., 2013a), further compounding the problem of the identity of CMNFV 22039. The close relationship that we recover between CMNFV 22039 and *Prenocephale* in our reduced strict consensus tree (Fig. 16B) is based on just a single trait (weakly pendant fourth trochanter of the femur), but without further knowledge of the distribution of this trait among pachycephalosaurs, we have correspondingly little confidence in the phylogenetic result. In fact, biogeographic considerations preclude such candidate genera as *Prenocephale*, *Homalocephale*, or *Wannanosaurus*, which are otherwise known only from Asia, and pachycephalosaurian genera are not yet known to span continents (Evans et al., 2021; Schott &

FIGURE 18. Life reconstruction of CMNFV 22039 in an environment typical of the upper Maastrichtian Frenchman Formation. Illustration by Kaitlin Lindblad. Used with permission.

Evans, 2016). However, this argument must not be pressed too hard, because some dinosaur genera are transcontinental (e.g., *Saurolophus* Brown, 1912). Within North America, taxa that pre-date the late Maastrichtian (e.g., *Acrotholus*, *Colepiocephale*, *Stegoceras*) are also unlikely due to their chronostratigraphic age.

If CMNFV 22039 pertains to a known taxon, the most likely candidates are *Pachycephalosaurus wyomingensis*, *Sp. buchholtzae*, *Sp. triregnum*, and *Sty. spinifer*, as they occur in chronostratigraphically correlative rocks of central North America, notably the Hell Creek Formation of Montana just to the south. Specimen CMNFV 22039 shares no overlapping material with the first three species, and, apart from size, it differs most notably from *Sty. spinifer* in the relatively longer preacetabular process of the ilium and the straight postacetabular process. Of the four aforementioned candidate species, only cf. *Sp. buchholtzae* has so far been described from the Frenchman Formation (Mallon et al., 2015), which gives some reason to think that CMNFV 22039 might be attributable to that species. However, more extensive sampling of the formation is clearly needed to clarify the nature of its faunal assemblage. As such, we prefer a taxonomically conservative approach and presently refer CMNFV 22039 to Pachycephalosauria indet.

Hindlimb Scaling

The condition of having relatively longer distal hindlimbs in bipeds typically confers enhanced running abilities (Carrano, 1999). Thus, a long-legged juvenile pachycephalosaur such as CMNFV 22039, while perhaps not absolutely faster than its adult counterparts (given its smaller body size), would nonetheless have benefited from a relative performance advantage, covering a distance equal to its own body length in less time. This advantage among small, immature growth forms is known as performance compensation (Carrier, 1996; Herrel & Gibb, 2006) and is common among vertebrates (e.g., Dial & Carrier, 2012; Dial & Young et al., 2010; Emerson, 1978). Among hadrosaurid dinosaurs, the hindlimbs of at least some species apparently grew isometrically (Mallon et al., 2023; Wosik et al., 2017). This observation led Mallon et al. (2023) to suggest that groups of young hadrosaurids, for which there is ample evidence (e.g., Joubarne et al., 2024; Scott et al., 2022; Wosik et al., 2020), might therefore have benefited instead from increased vigilance and/or the dilution effect, thereby compensating for an inability to outrun hopeful predators. If there is any validity to this argument, it might also be applied to suggest, conversely, that juvenile pachycephalosaurs, which apparently did benefit from ontogenetic performance compensation, may have foraged alone. To date, there are no known pachycephalosaurian bonebeds, despite a relative abundance of frontoparietal domes. Without more positive evidence, however, the matter of pachycephalosaur gregariousness is highly speculative.

The suggested negative allometry of the distal hindlimbs in pachycephalosaurids contrasts with the positive allometry of the frontoparietal dome (Chapman et al., 1981; Evans et al., 2013a; Horner & Goodwin, 2009; Schott et al., 2011). Use of the dome in agonistic head- or flank-butting is broadly accepted (e.g., Carpenter, 1997; Peterson et al., 2013; Snively & Theodor, 2011; Sues & Galton, 1987; but see Goodwin & Horner [2004] and Horner et al. [2022] for an alternative view), and Moore et al. (2022) recently cited a suite of postcranial adaptations

that might have facilitated this behaviour in adults. Such adaptations include modifications of the vertebrae and pelvis to limit lateral flexion of the spine, and relatively reduced hindlimbs to lower the center of gravity for enhanced stability during impact. Dome-less juvenile pachycephalosaurids, being incapable of such head-butting behavior, would not have benefited from this lowered center of gravity. Thus, on the agonistic combat hypothesis, negative allometry of the hindlimbs is expected.

CONCLUSIONS

We identify CMNFV 22039 as an early juvenile pachycephalosaur, likely the youngest postcranium known so far. Relevant pachycephalosaurian traits include: (1) a double ridge-and-groove articulation on the pre- and postzygapophyses of the dorsal neural arches; (2) a medial flange on the postacetabular process of the ilium; and (3) a highly reduced pubis that contributes only minimally to the acetabular margin (Maryańska et al., 2004). A more precise taxonomic identity could not be determined due to a lack of diagnostic material; however, *Sphaerotholus buchholtzae* is a likely candidate, based on concordance in stratigraphic age, geographic location, and non-conflicting postcranial character traits. The early juvenile life stage of CMNFV 22039 is supported by: (1) its small size; (2) unfused neurocentral sutures of the vertebrae; (3) a grainy, porous surface texture of the bones; (4) histological analysis showing a rapidly growing woven bone of the tibia and fibula; and (5) a lack of any growth annuli.

Although our cladistic analysis included new postcranial characters to help resolve taxonomic relationships among pachycephalosaurs, phylogenetic resolution nevertheless remains low without resorting to additional data manipulation (e.g., character weighting, deletion of unstable taxa). While missing data remain an important issue for pachycephalosaur phylogenetics, the addition of postcranial characters may lead to increased character conflict, evidenced by the slightly lower consistency and retention indices we recover compared with some other recent analyses (e.g., Woodruff et al., 2023). The possibility of conflict between cranial and postcranial characters is of considerable interest. Some studies (Carpenter, 1997; Moore et al., 2022; Sues & Galton, 1987) have argued that the pachycephalosaurian skeleton, including the head and postcranium, effectively operated as a single functional unit, adapted to head-butting behavior. Modular variation in the skeleton may argue against this hypothesis and therefore should be investigated. By contrast, evidence for a probable negative ontogenetic allometry of the pachycephalosaur hindlimb presented in this study aligns with the agonistic head-butting hypothesis.

ACKNOWLEDGMENTS

We thank A. McDonald, S.E. Pan, S. Rufolo, and C. Tsogtbaatar for providing digital models and photographs of specimens. We also thank K. Seymour and B. Iwama for allowing access to the collection facilities of the Royal Ontario Museum. Special thanks to C. Woodruff for his aid in creating and photographing histological sections. Valuable field assistance was provided by B. Peterson, M. Peterson, and G. Danis. Finally, thanks to the Willi Hennig Society for providing the free TNT software used in this study. Project funding was provided by the Natural Sciences and Engineering Research Council of Canada (to DCE, JCM, and RTP), the Dale Patten Memorial Fund at the Canadian Museum of Nature, and the Dinosaur Research Institute (to BRSM).

AUTHOR CONTRIBUTIONS

BRSM, DCE, and JCM designed the project. BRSM, DCE, and JCM were responsible for data collection. BRSM, DCE, and JCM drafted the manuscript and analyzed the data. All authors edited the manuscript.

DATA AVAILABILITY

All data necessary to replicate the findings of this study are available either in this paper or in the supplementary files provided on MorphoBank (https://www.morphobank.org/project/5718/overview). 3D models generated for this study can be found at MorphoSource: https://www.morphosource.org/projects/000731298.

DISCLOSURE STATEMENT

No potential conflict of interest was reported by the author(s).

SUPPLEMENTARY FILES

SupplementaryFile1.tif: high resolution image of the histological cross section of the tibia and fibula of CMNFV 22039.

SupplementaryFile2.tnt: morphological character matrix used for phylogenetic analysis (TNT format).

SupplementaryFile3.xlsx: hindlimb measurement data used to develop ternary diagram.

SupplementaryFile4.tre: most parsimonious trees and strict consensus tree resulting from equal weighting parsimony analysis.

SupplementaryFile5.tre: most parsimonious trees and strict consensus tree resulting from implied weighting parsimony analysis.

SupplementaryFile6.tre: reduced strict consensus trees resulting from deletion of unstable taxa.

LITERATURE CITED

Averianov, A. O., Voronkevich, A. V., Leshchinskiy, S. V., & Fayngertz, A. V. (2006). A ceratopsian dinosaur *Psittacosaurus sibiricus* from the Early Cretaceous of West Siberia, Russia and its phylogenetic relationships. *Journal of Systematic Palaeontology*, *4*(4), 359–395. https://doi.org/10.1017/S1477201906001933

Bakker, R. T., Sullivan, R. M., Porter, V., Larson, P., & Saulsbury, S. J. (2006). *Dracorex hogwartsia*, n. gen., n. sp., a spiked, flat-headed pachycephalosaurid dinosaur from the Upper Cretaceous Hell Creek Formation of South Dakota. *New Mexico Museum of Natural History Science Bulletin*, *35*, 331–345.

Bamforth, E. L. (2013). Paleoecology and paleoenvironmental trends immediately prior to the end-Cretaceous extinction in the latest Maastrichtian (66 Ma) Frenchman Formation, Saskatchewan, Canada. Ph.D. thesis. McGill University.

Bamforth, E. L., Button, C. L., & Larsson, H. C. E. (2014). Paleoclimate estimates and fire ecology immediately prior to the end-Cretaceous mass extinction in the Frenchman Formation (66 Ma), Saskatchewan, Canada. *Palaeogeography, Palaeoclimatology, Palaeoecology*, *401*, 96–110. https://doi.org/10.1016/j.palaeo.2014.02.020

Boyd, C. A., Brown, C. M., Scheetz, R. D., & Clarke, J. A. (2009). Taxonomic revision of the basal neornithischian taxa *Thescelosaurus* and *Bugenasaura*. *Journal of Vertebrate Paleontology*, *29*(3), 758–770. https://doi.org/10.1671/039.029.0328

Brochu, C. A. (1996). Closure of neurocentral sutures during crocodilian ontogeny: Implications for maturity assessment in fossil archosaurs. *Journal of Vertebrate Paleontology*, *16*(1), 49–62. https://doi.org/10.1080/02724634.1996.10011283

Brown, B. (1912). A crested dinosaur from the Edmonton Cretaceous. *Bulletin of the American Museum of Natural History*, *31*, 131.

Brown, B., & Schlaiker, E. M. (1943). A study of the troödont dinosaurs with the description of a new genus and four new species. *Bulletin of the American Museum of Natural History*, *82*, 121–149.

Brown, C. M. (2009). *Thescelosaurus* (Dinosauria: Ornithischia) and related taxa from the Late Cretaceous of Alberta and Saskatchewan [Unpublished doctoral dissertation]. University of Toronto.

Brown, C. M., Boyd, C. A., & Russell, A. P. (2011). A new basal ornithopod dinosaur (Frenchman Formation, Saskatchewan, Canada) and implications for late Maastrichtian ornithischian diversity in North America. *Zoological Journal of the Linnean Society*, *163*(4), 1157–1198. https://doi.org/10.1111/j.1096-3642.2011.00735.x

Brown, C. M., Evans, D. C., Ryan, M. J., & Russell, A. P. (2013). New data on the diversity and abundance of small-bodied ornithopods (Dinosauria, Ornithischia) from the Belly River Group (Campanian) of Alberta. *Journal of Vertebrate Paleontology*, *33*(3), 495–520. https://doi.org/10.1080/02724634.2013.746229

Brown, C. M., Ryan, M. J., Evans, D. C., Bininda-Emonds, O. R. P., Powell, G. L., Jamniczky, H. A., Bauer, A. M., & Theodor, J. (2015). A census of Canadian dinosaurs: More than a century of discovery. In *All Animals Are Interesting: A Festschrift in Honour of Anthony P. Russell* (pp. 151–209). BIS Verlag.

Butler, R. J., & Sullivan, R. M. (2009). The phylogenetic position of the ornithischian dinosaur *Stenopelix valdensis* from the Lower Cretaceous of Germany and the early fossil record of Pachycephalosauria. *Acta Palaeontologica Polonica*, *54*(1), 21–34. https://doi.org/10.4202/app.2009.0104

Butler, R. J., & Zhao, Q. (2009). The small-bodied ornithischian dinosaurs *Micropachycephalosaurus hongtuyanensis* and *Wannanosaurus yansiensis* from the Late Cretaceous of China. *Cretaceous Research*, *30*(1), 63–77. https://doi.org/10.1016/j.cretres.2008.03.002

Campione, N.E. (2020). MASSTIMATE: Body mass estimation equations for vertebrates (Version 2.0-1) [R package]. Retrieved from https://CRAN.R-project.org/package=MASSTIMATE.

Carpenter, K. (1997). Agonistic behavior in pachycephalosaurs (Ornithischia, Dinosauria); a new look at head-butting behavior. *Rocky Mountain Geology*, *32*(1), 19–25.

Carrano, M. T. (1999). What, if anything, is a cursor? Categories versus continua for determining locomotor habit in mammals and dinosaurs. *Journal of Zoology*, *247*(1), 29–42. https://doi.org/10.1111/j.1469-7998.1999.tb00190.x

Carrier, D. R. (1996). Ontogenetic limits on locomotor performance. *Physiological Zoology*, *69*(3), 467–488. https://doi.org/10.1086/physzool.69.3.30164211

Castanet, J., Rogers, K. C., Cubo, J., & Jacques-Boisard, J. (2000). Periosteal bone growth rates in extant ratites (ostriche and emu). Implications for assessing growth in dinosaurs. *Comptes Rendus de l'Académie des Sciences - Series III - Sciences de la Vie*, *323*(6), 543–550. https://doi.org/10.1016/S0764-4469(00)00181-5

Catuneanu, O., & Sweet, A. R. (1999). Maastrichtian–Paleocene foreland-basin stratigraphies, western Canada: A reciprocal sequence architecture. *Canadian Journal of Earth Sciences*, *36*(5), 685–703. https://doi.org/10.1139/e98-018

Chapman, R. E., Galton, P. M., Sepkoski Jr J. J., & Wall, W. P. (1981). A morphometric study of the cranium of the pachycephalosaurid dinosaur *Stegoceras*. *Journal of Paleontology*, *55*, 608–618.

Chinzorig, T., Takasaki, R., Yoshida, J., Tucker, R. T., Buyantegsh, B., Mainbayar, B., Tsogtbaatar, K., & Zanno, L. E. (2025). A domed pachycephalosaur from the Early Cretaceous of Mongolia. *Nature*, https://doi.org/10.1038/s41586-025-09213-6

Chure, D., Turner, C., & Peterson, F. (1994). An embryo of *Camptosaurus* from the Morrison Formation (Jurassic, Middle Tithonian) in Dinosaur National Monument, Utah. In K. Carpenter, K. F. Hirsch, & J. R. Horner (Eds.), *Dinosaur Eggs and Babies* (pp. 298–311). Cambridge University Press.

Curry Rogers, K., Whitney, M., D'Emic, M., & Bagley, B. (2016). Precocity in a tiny titanosaur from the Cretaceous of Madagascar. *Science*, *352*(6284), 450–453. https://doi.org/10.1126/science.aaf1509

de Margerie, E., Cubo, J., & Castanet, J. (2002). Bone typology and growth rate: testing and quantifying 'Amprino's rule' in the mallard (*Anas platyrhynchos*). *Comptes Rendus. Biologies*, *325*(3), 221–230. https://doi.org/10.1016/S1631-0691(02)01429-4

de Rooij, J., Vintges, M. Q., Zuidwijk, T., Heerkens, C. T., & Schulp, A. S. (2023). Quantification of bone surface textures: exploring a new method of ontogenetic ageing. *Journal of Analytical Science and Technology*, *14*(1), 49. https://doi.org/10.1186/s40543-023-00413-1

Dial, T. R., & Carrier, D. R. (2012). Precocial hindlimbs and altricial forelimbs: partitioning ontogenetic strategies in mallard ducks *(Anas platyrhynchos)*. *Journal of Experimental Biology*, *215*, 3703–3710. https://doi.org/10.1242/jeb.057380

Dieudonné, P. E., Cruzado-Caballero, P., Godefroit, P., & Tortosa, T. (2021). A new phylogeny of cerapodan dinosaurs. *Historical Biology*, *33*(10), 2335–2355. https://doi.org/10.1080/08912963.2020.1793979

Eberth, D. A., & Kamo, S. L. (2019). First high-precision U–Pb CA–ID–TIMS age for the Battle Formation (Upper Cretaceous), Red Deer River valley, Alberta, Canada: Implications for ages, correlations, and dinosaur biostratigraphy of the Scollard, Frenchman, and Hell Creek formations. *Canadian Journal of Earth Sciences*, *56*(10), 1041–1051. https://doi.org/10.1139/cjes-2018-0098

Emerson, S. B. (1978). Allometry and jumping in frogs: Helping the twain to meet. *Evolution*, *32*(3), 551–564. https://doi.org/10.1111/j.1558-5646.1978.tb04598.x

Evans, D. C., Brown, C. M., Ryan, M. J., & Tsogtbaatar, K. (2011). Cranial ornamentation and ontogenetic status of *Homalocephale calathocercos* (Ornithischia: Pachycephalosauria) from the Nemegt Formation, Mongolia. *Homalocephale calathocercos Journal of Vertebrate Paleontology*, *31*(1), 84–92. https://doi.org/10.1080/02724634.2011.546287

Evans, D. C., Brown, C. M., You, H., & Campione, N. E. (2021). Description and revised diagnosis of Asia's first recorded pachycephalosaurid, *Sinocephale bexelli* gen. nov., from the Upper Cretaceous of Inner Mongolia, China. *Canadian Journal of Earth Sciences*, *58*(10), 981–992. https://doi.org/10.1139/cjes-2020-0190

Evans, D., Campione, N., Brink, K., Schott, R., & Brown, C. (2013a). Wasted youth: the importance of ontogenetically equivalent semaphoronts in dinosaur phylogenetic systematics. *Journal of Vertebrate Paleontology, Program and Abstracts*, 2013, 123.

Evans, D. C., Schott, R. K., Larson, D. W., Brown, C. M., & Ryan, M. J. (2013b). The oldest North American pachycephalosaurid and the hidden diversity of small-bodied ornithischian dinosaurs. *Nature Communications*, https://doi.org/10.1038/ncomms2749

Fastovsky, D., Weishampel, D., Watabe, M., Barsbold, R., Tsogtbaatar, K., & Narmandakh, P. (2011). A nest of *Protoceratops andrewsi* (Dinosauria, Ornithischia). *Journal of Paleontology*, *85*(6), 1035–1041. https://doi.org/10.1666/11-008.1

Fonseca, A. O., Reid, I. J., Venner, A., Duncan, R. J., Garcia, M. S., & Müller, R. T. (2024). A comprehensive phylogenetic analysis on early ornithischian evolution. *Journal of Systematic Palaeontology*, *22*(1), 2346577. https://doi.org/10.1080/14772019.2024.2346577

Francillon-Vieillot, H., de Buffrenil, V., Castanet, J., Géraudie, J., Meunier, F.-J., Sire, J.-Y., Zylbergberg, L., & de Ricqlès, A. (1990). Microstructure and mineralization of vertebrate skeletal tissues. In J. G. Carter (Ed.), *Skeletal Biomineralization: Patterns, Processes and Evolutionary Trends* (pp. 471–530). Van Nostrand Reinhold.

Fraser, F. J., McLearn, F. H., Russell, L. S., Warren, P. S., & Wickenden, R. T. D. (1935). Geology of southern Saskatchewan. *Geological Survey of Canada Memoirs*, *176*, 1–137.

Furnival, G. M. (1946). Cypress Lake map-area, Saskatchewan. *Geological Survey of Canada Memoirs*, *242*, 1–161.

Galton, P. M. (2014). Notes on the postcranial anatomy of the heterodontosaurid dinosaur *Heterodontosaurus tucki*, a basal ornithischian from the Lower Jurassic of South Africa. *Revue de Paléobiologie*, *33*(1), 97–141.

Gilmore, C. W. (1915). Osteology of *Thescelosaurus*, an orthopodous dinosaur from the Lance Formation of Wyoming. *Proceedings of the United States National Museum*, *49*(2127), 591–616. https://doi.org/10.5479/si.00963801.49-2127.591

Gilmore, C. W. (1924). On *Troodon validus*: An orthopodus dinosaur from the Belly River Cretaceous of Alberta, Canada. *University of Alberta, Department of Geology, Bulletin*, *1*, 1–58.

Goloboff, P. A., Carpenter, J., Arias, S., & Miranda, D. (2008). Weighting against homoplasy improves phylogenetic analysis of morphological data sets. *Cladistics*, *24*(5), 758–773. https://doi.org/10.1111/j.1096-0031.2008.00209.x

Goloboff, P. A., & Morales, M. E. (2023). TNT version 1.6, with a graphical interface for MacOS and Linux, including new routines in parallel. *Cladistics*, *39*(2), 144–153. https://doi.org/10.1111/cla.12524

Goloboff, P. A., Torres, A., & Arias, J. S. (2018). Weighted parsimony outperforms other methods of phylogenetic inference under models appropriate for morphology. *Cladistics*, *34*(4), 407–437. https://doi.org/10.1111/cla.12205

Goodwin, M. B., & Horner, J. R. (2004). Cranial histology of pachycephalosaurs (Ornithischia: Marginocephalia) reveals transitory structures inconsistent with head-butting behavior. *Paleobiology*, *30*(2), 253–267. https://doi.org/10.1666/0094-8373(2004)030<0253:chopom>2.0.co;2

Griffin, C. T., Stocker, M. R., Collearny, C., Stefanic, C. M., Lessner, E. J., Riegler, M., Formoso, K., Koeller, K., & Nesbitt, S. J. (2021). Assessing ontogenetic maturity in extinct saurian reptiles. *Biological Reviews*, *96*(2), 470–525. https://doi.org/10.1111/brv.12666

Herrel, A., & Gibb, A. C. (2006). Ontogeny of performance in vertebrates. *Physiological and Biochemical Zoology*, *79*(1), 1–6. https://doi.org/10.1086/498196

Hoffman, R., & Sander, P. M. (2014). The first juvenile specimens of *Plateosaurus engelhardti* from Frick, Switzerland: isolated neural arches and their implications for developmental plasticity in a basal sauropodomorph. *PeerJ*, *2*, e458. https://doi.org/10.7717/peerj.458

Hone, D. W. E., Farke, A. A., & Wedel, M. J. (2016). Ontogeny and the fossil record: what, if anything, is an adult dinosaur? *Biology Letters*, *12*(2), 20150947. https://doi.org/10.1098/rsbl.2015.0947

Horner, J. R., & Currie, P. J. (1994). Embryonic and neonatal morphology and ontogeny of a new species of *Hypacrosaurus* (Ornithischia: Lambeosaurinae) from Montana and Alberta. In K. Carpenter, K.F. Hirsch, & J. R. Horner (Eds.), *Dinosaur Eggs and Babies* (pp. 312–336). Cambridge University Press.

Horner, J. R., & Goodwin, M. B. (2009). Extreme cranial ontogeny in the Upper Cretaceous dinosaur *Pachycephalosaurus*. *PLoS One*, *4*(10), e7626. https://doi.org/10.1371/journal.pone.0007626

Horner, J. R., Goodwin, M. B., & Evans, D. C. (2022). A new pachycephalosaurid from the Hell Creek Formation, Garfield County, Montana, U.S.A. *Journal of Vertebrate Paleontology*, *42*(4), e2190369. https://doi.org/10.1080/02724634.2023.2190369

Horner, J. R., & Makela, R. (1979). Nest of juveniles provides evidence of family structure among dinosaurs. *Nature*, *282*(5736), 296–298. https://doi.org/10.1038/282296a0

Horner, J. R., Padian, K., & de Ricqlès, A. (2001). Comparative osteohistology of some embryonic and perinatal archosaurs: developmental and behavioral implications for dinosaurs. *Paleobiology*, *27*(1), 39–58. https://doi.org/10.1666/0094-8373(2001)027<0039:coosea>2.0.co;2

Horner, J. R., & Weishampel, D. B. (1988). A comparative embryological study of two ornithischian dinosaurs. *Nature*, *332*(6161), 256–57. https://doi.org/10.1038/332256a0

Jacobs, L. L., Winkler, D. A., Murry, P. A., & Maurice, J. M. (1994). A nodosaurid scuteling from the Texas shore of the Western Interior Seaway. In K. Carpenter, K. F. Hirsch, & J. R. Horner (Eds.), *Dinosaur Eggs and Babies* (pp. 337–346). Cambridge University Press.

Joubarne, T., Therrien, F., & Zelenitsky, D. K. (2024). Evidence of age segregation behavior in *Hypacrosaurus stebingeri* (Hadrosauridae: Lambeosaurinae) based on the taphonomic comparison of bonebeds from the Upper Cretaceous (upper Campanian) Oldman Formation of southernmost Alberta (Canada) and Two Medicine Formation of Montana (USA). *Palaeogeography, Palaeoclimatology, Palaeoecology*, *653*, 112416. https://doi.org/10.1016/j.palaeo.2024.112416

Irmis, R. B. (2007). Axial skeleton ontogeny in the Parasuchia (Archosauria: Pseudosuchia) and its implications for ontogenetic determination in archosaurs. *Journal of vertebrate Paleontology*, *27*(2), 350–361. https://doi.org/10.1671/0272-4634(2007)27[350:ASOITP]2.0.CO;2>

Kupsch, W. O. (1957). Frenchman Formation of eastern Cypress Hills, Saskatchewan, Canada. *Geological Society of America Bulletin*, *68*(4), 413–420. https://doi.org/10.1130/0016-7606(1957)68[413:FFOECH]2.0.CO;2

Lambe, L. M. (1902). New genera and species from the Belly River Series (mid-Cretaceous). *Contributions to Canadian Palaeontology*, *3*(Part II), 25–81.

Lamm, E.-T., & Werning, S. (2013). *Bone Histology of Fossil Tetrapods: Advancing Methods, Analysis, and Interpretation*. University of California Press.

Leidy, J. (1856). Notices of the remains of extinct reptiles and fishes discovered by Dr. FV Hayden in the bad-lands of the Judith River, Nebraska Territory. *Academy of Natural Sciences, Philadelphia, Proceedings*, *8*, 72–73.

Madzia, D., Arbour, V. M., Boyd, C. A., Farke, A. A., Cruzado-Caballero, P., & Evans, D. C. (2021). The phylogenetic nomenclature of ornithischian dinosaurs. *PeerJ*, *9*, e12362. https://doi.org/10.7717/peerj.12362

Mallon, J. C., & Evans, D. C. (2014). Taphonomy and habitat preference of North American pachycephalosaurids (Dinosauria, Ornithischia). *Lethaia*, *47*(4), 567–578. https://doi.org/10.1111/let.12082

Mallon, J. C., Evans, D. C., Tokaryk, T. T., & Currie, M. L. (2015). First pachycephalosaurid (Dinosauria: Ornithischia) from the Frenchman Formation (upper Maastrichtian) of Saskatchewan, Canada. *Cretaceous Research*, *56*, 426–431. https://doi.org/10.1016/j.cretres.2015.06.005

Mallon, J. C., Evans, D. C., Zhang, Y., & Xing, H. (2023). Rare juvenile material constrains estimation of skeletal allometry in *Gryposaurus notabilis* (Dinosauria: Hadrosauridae). *The Anatomical Record*, *306*(7), 1646–1668. https://doi.org/10.1002/ar.25021

Mallon, J. C., Roloson, M., Bamforth, E. L., Scannella, J. B., & Ryan, M. J. (2025). The Canadian fossil record supports anagenesis in *Triceratops* (Ornithischia, Ceratopsia). *Canadian Journal of Earth Sciences*, *62*(7), 1222–1372. https://doi.org/10.1139/cjes-2024-0170

Marsh, O. C. (1890). Description of new dinosaurian reptiles. *American Journal of Science*, *33-39*(229), 81–86. https://doi.org/10.2475/ajs.s3-39.229.81

Maryańska, T., Chapman, R. E., & Weishampel, D. B. (2004). Pachycephalosauria. In D. B. Weishampel, P. Dodson, & H. Osmólska (Eds.), *The Dinosauria* (pp. 465–477). University of California Press.

Maryańska, T., & Osmólska, H. (1974). Pachycephalosauria, a new suborder of ornithischian dinosaurs. *Palaeontologia Polonica*, *26*, 133–182.

McIver, E. E. (2002). The paleoenvironment of *Tyrannosaurus rex* from southwestern Saskatchewan, Canada. *Canadian Journal of Earth Sciences*, *39*(2), 207–221. https://doi.org/10.1139/e01-073

Moore, B. R., Roloson, M. J., Currie, P. J., Ryan, M. J., Patterson, R. T., & Mallon, J. C. (2022). The appendicular myology of *Stegoceras validum* (Ornithischia: Pachycephalosauridae) and implications for the head-butting hypothesis. *PLoS One*, *17*(9), e0268144. https://doi.org/10.1371/journal.pone.0268144

Mossop, G., & Shetsen, I. (1994). *Geological Atlas of the Western Canada Sedimentary Basin*. Canadian Society of Petroleum Geologists and Alberta Research Council.

Osborn, H. F. (1923). Two Lower Cretaceous dinosaurs from Mongolia. *American Museum Novitates*, *95*, 1–10.

Perle, A., Maryańska, T., & Osmólska, H. (1982). *Goyocephale lattimorei* gen. et sp. nov., a new flat-headed pachycephalosaur (Ornithischia, Dinosauria) from the Upper Cretaceous of Mongolia. *Acta Palaeontologica Polonica*, *27*, 115–132.

Persons, W. S., & Currie, P. J. (2020). The anatomical and functional evolution of the femoral fourth trochanter in ornithischian dinosaurs. *The Anatomical Record*, *303*(4), 1146–1157. https://doi.org/10.1002/ar.24094

Peterson, J. E., Dischler, C., & Longrich, N. R. (2013). Distributions of cranial pathologies provide evidence for head-butting in dome-headed dinosaurs (Pachycephalosauridae). *PLoS One*, *8*(7), e68620. https://doi.org/10.1371/journal.pone.0068620

Prieto-Márquez, A., Erickson, G. A., & Ebersole, J. A. (2016a). A primitive hadrosaurid from southeastern North America and the origin and early evolution of 'duck-billed' dinosaurs. *Journal of Vertebrate Paleontology*, *36*(e1054495), https://doi.org/10.1080/02724634.2015.1054495

Prieto-Márquez, A., Erickson, G. A., & Ebersole, J. A. (2016b). Anatomy and osteohistology of the basal hadrosaurid dinosaur *Eotrachodon* from the uppermost Santonian (Cretaceous) of southern Appalachia. *PeerJ*, *4*, e1872. https://doi.org/10.7717/peerj.1872

Redelstorff, R., & Sander, P. M. (2009). Long and girdle bone histology of *Stegosaurus*: implications for growth and life history. *Journal of Vertebrate Paleontology*, *29*(4), 1087–1099. https://doi.org/10.1671/039.029.0420

Russell, D. (1973). Field notes. *Canadian Museum of Nature Archives*.

Russell, D., & Manabe, M. (2002). The Hell Creek Formation and the Cretaceous-Tertiary boundary in the northern Great Plains: An integrated continental record of the end of the Cretaceous. *Geological Society of America*, *361*, 169–176. https://doi.org/10.1130/0-8137-2361-2.169

Ryan, W. B. F., Carbotte, S. M., Coplan, J., O'Hara, S., Melkonian, A., Arko, R., Weissel, R. A., Ferrini, V., Goodwillie, A., Nitsche, F., Bonczkowski, J., & Zemsky, R. (2009). Global multi-resolution topography synthesis. *Geochemistry, Geophysics, Geosystems*, *10*(3), Q03014. https://doi.org/10.1029/2008GC002332

Schott, R. K., & Evans, D. C. (2016). Cranial variation and systematics of *Foraminacephale brevis* gen. nov. and the diversity of pachycephalosaurid dinosaurs (Ornithischia: Cerapoda) in the Belly River Group of Alberta, Canada. *Zoological Journal of the Linnean Society*, *179*(4), 865–906. https://doi.org/10.1111/zoj.12465

Schott, R. K., Evans, D. C., Goodwin, M. B., Horner, J. R., & Brown, C. M. (2011). Cranial ontogeny in *Stegoceras validum* (Dinosauria: Pachycephalosauria): A quantitative model of pachycephalosaur dome growth and variation. *PLoS One*, *6*(6), https://doi.org/10.1371/journal.pone.0021092

Scott, E. E., Chiba, K., Fanti, F., Saylor, B. Z., Evans, D. C., & Ryan, M. J. (2022). Taphonomy of a monodominant *Gryposaurus* sp. bonebed from the Oldman Formation (Campanian) of Alberta, Canada. *Canadian Journal of Earth Sciences*, *59*(6), 389–405. https://doi.org/10.1139/cjes-2020-0200

Sereno, P. C. (1987). The ornithischian dinosaur *Psittacosaurus* from the Lower Cretaceous of Asia and the relationships of the Ceratopsia [Unpublished doctoral dissertation]. Columbia University.

Sereno, P. C. (1997). The origin and evolution of dinosaurs. *Annual Review of Earth and Planetary Sciences*, *25*(1), 435–489. https://doi.org/10.1146/annurev.earth.25.1.435

Sereno, P. C., Shichin, C., Zhengwu, C., & Chenggang, R. (1988). *Psittacosaurus meileyingensis* (Ornithischia: Ceratopsia), a new psittacosaur from the Lower Cretaceous of northeastern China. *Journal of Vertebrate Paleontology*, *8*(4), 366–377. https://doi.org/10.1080/02724634.1988.10011725

Slowiak, J., Tereshchenko, V. S., & Fostowicz-Frelik, Ł. (2019). Appendicular skeleton of *Protoceratops andrewsi* (Dinosauria, Ornithischia): comparative morphology, ontogenetic changes, and the implications for non-ceratopsid ceratopsian locomotion. *PeerJ*, *7*, e7324. https://doi.org/10.7717/peerj.7324

Snively, E., & Theodor, J. M. (2011). Common functional correlates of head-strike behavior in the pachycephalosaur *Stegoceras validum* (Ornithischia, Dinosauria) and combative artiodactyls. *PLoS One*, *6*(6), e21422. https://doi.org/10.1371/journal.pone.0021422

Storer, J. E. (1989). *Geological History of Saskatchewan*. Saskatchewan Museum of Natural History.

Sues, H. D., & Galton, P. M. (1982). The systematic position of *Stenopelix valdensis* (Reptilia: Ornithischia) from the Wealden of northwestern Germany. *Palaeontographica*, *178*, 183–190.

Sues, H. D., & Galton, P. M. (1987). Anatomy and classification of the North American Pachycephalosauria (Dinosauria: Ornithischia). *Palaeontographica Abt. A*, *198*, 1–40.

Sullivan, R. M. (2006). A taxonomic review of the Pachycephalosauridae (Dinosauria; Ornithischia). *New Mexico Museum of Natural History and Science Bulletin*, *35*, 347–365.

Tokaryk, T. T. (1997). First evidence of juvenile ceratopsians (Reptilia: Ornithischia) from the Frenchman Formation (late Maastrichtian) of Saskatchewan. *Canadian Journal of Earth Sciences*, *34*(10), 1401–1404. https://doi.org/10.1139/e17-112

Tokaryk, T. T. (2009). Head-hunting in Saskatchewan: The history of *Triceratops*. *Frenchman Formation Terrestrial Ecosystem Conference. Eastend, Saskatchewan: Royal Saskatchewan Museum Contribution to Science*, *12*, 61–62.

Tokaryk, T. T., & Brinkman, D. (2009). Turtles from the Frenchman Formation and latitudinal patterns of distribution of turtles in the late Maastrichtian. *Gaffney Turtle Symposium.* Royal Tyrrell Museum, Drumheller, Alberta, 178–179.

Tokaryk, T. T., & Bryant, H. N. (2004). The fauna from the *Tyrannosaurus rex* excavation, Frenchman Formation (late Maastrichtian), Saskatchewan summary of investigations. *Saskatchewan Geological Survey, Saskatchewan Industry Resources, Misc. Rep*, *1*, 1–12.

Tokaryk, T. T., & James, P. C. (1989). *Cimolopteryx* sp. (Aves, Charadriiformes) from the Frenchman Formation (Maastrichtian), Saskatchewan. *Canadian Journal of Earth Sciences*, *26*(12), 2729–2730. https://doi.org/10.1139/e89-233

Tumarkin-Deratzian, A. R., Vann, D. R., & Dodson, P. (2006). Bone surface texture as an ontogenetic indicator in long bones of the Canada goose *Branta canadensis* (Anseriformes: Anatidae). *Zoological Journal of the Linnean society*, *148*(2), 133–168. https://doi.org/10.1111/j.1096-3642.2006.00232.x

Williamson, T. E., & Brusatte, S. L. (2016). Pachycephalosaurs (Dinosauria: Ornithischia) from the Upper Cretaceous (upper Campanian) of New Mexico: A reassessment of *Stegoceras novomexicanum*. *Cretaceous Research*, *62*, 29–43. https://doi.org/10.1016/j.cretres.2016.01.012

Williamson, T. E., & Carr, T. D. (2003). A new genus of derived pachycephalosaurian from western North America. *Journal of Vertebrate Paleontology*, *22*(4), 779–801. https://doi.org/10.1671/0272-4634(2002)022[0779:ANGODP]2.0.CO;2

Woodruff, D. C., Schott, R. K., & Evans, D. C. (2023). Two new species of small-bodied pachycephalosaurine (Dinosauria, Marginocephalia) from the uppermost Cretaceous of North America suggest hidden diversity in well-sampled formations. *Papers in Palaeontology*, *9*(6), e1535. https://doi.org/10.1002/spp2.1535

Wosik, M., Chiba, K., Therrien, F., & Evans, D. C. (2020). Testing size–frequency distributions as a method of ontogenetic aging: a life-history assessment of hadrosaurid dinosaurs from the Dinosaur Park Formation of Alberta, Canada, with implications for hadrosaurid paleoecology. *Paleobiology*, *46*(3), 379–404. https://doi.org/10.1017/pab.2020.2

Wosik, M., Goodwin, M. B., & Evans, D. C. (2017). A nestling-sized skeleton of *Edmontosaurus* (Ornithischia, Hadrosauridae) from the Hell Creek Formation of northeastern Montana, U.S.A., with an analysis of ontogenetic limb allometry. *Journal of Vertebrate Paleontology*, *37*(6), e1398168. https://doi.org/10.1080/02724634.2017.1398168

Young, J. W., Fernández, D., & Fleagle, J. G. (2010). Ontogeny of long bone geometry in capuchin monkeys (*Cebus albifrons* and *Cebus apella*): implications for locomotor development and life history. *Biology Letters*, *6*(2), 197–200. https://doi.org/10.1098/rsbl.2009.0773

Handling Editor: Amy Balanoff.
Phylogenetics Editor: Pedro Godoy.